THE JOURNAL OF BIOLOGICAL CHEMISTRY VOL. 291, NO. 24, pp. 12821–12837, June 10, 2016

Presenilin 1 and Presenilin 2 Target γ-Secretase Complexes to Distinct Cellular Compartments*[S]

Received for publication, December 4, 2015, and in revised form, April 6, 2016 Published, JBC Papers in Press, April 8, 2016, DOI 10.1074/jbc.M115.708297

Xavier Meckler and Frédéric Checler[1]

From the Université de Nice Sophia-Antipolis, Institut de Pharmacologie Moléculaire et Cellulaire CNRS UMR7275, Laboratoire d'Excellence Distalz, Sophia-Antipolis, 06560 Valbonne, France

γ-Secretase complexes achieve the production of amyloid peptides playing a key role in Alzheimer disease. These proteases have many substrates involved in important physiological functions. They are composed of two constant subunits, nicastrin and PEN2, and two variable ones, presenilin (PS1 or PS2) and APH1 (APH1aL, APH1aS, or APH1b). Whether the composition of a given γ-secretase complex determines a specific cellular targeting remains unsolved. Here we combined a bidirectional inducible promoter and 2A peptide technology to generate constructs for the temporary, stoichiometric co-expression of six different combinations of the four γ-secretase subunits including EGFP-tagged nicastrin. These plasmids allow for the formation of functional γ-secretase complexes displaying specific activities and maturations. We show that PS1-containing γ-secretase complexes were targeted to the plasma membrane, whereas PS2-containing ones were addressed to the *trans*-Golgi network, to recycling endosomes, and, depending on the APH1-variant, to late endocytic compartments. Overall, these novel constructs unravel a presenilin-dependent subcellular targeting of γ-secretase complexes. These tools should prove useful to determine whether the cellular distribution of γ-secretase complexes contributes to substrate selectivity and to delineate regulations of their trafficking.

γ-Secretase complexes were mainly characterized through their association with Alzheimer disease (AD)[2] as they achieve the proteolytic cleavages of the amyloid precursor protein (APP) leading to the release of amyloid peptides (Aβs), which are considered to play a central role in the neurodegenerative process (1). The inhibition of γ-secretase activity was therefore regarded as a potential therapy for AD. However, clinical trials of γ-secretase inhibitors were halted because of increased occurrences of adverse effects in treated patients, including skin cancers and even a worsening of cognitive function (2, 3). These undesired consequences are probably due to the broad spectrum of γ-secretase inhibitors that are blocking the processing of not only APP, but also many other γ-secretase substrates. Indeed, numerous transmembrane proteins (up to 90 to date), including Notch, have been identified as γ-secretase substrates and are implicated in important signaling functions regulating cell fate, adhesion, migration, neurite outgrowth, or synaptogenesis (for reviews see Refs. 4 and 5). Research efforts are currently under way to develop alternative strategies to specifically inhibit/modulate γ-secretase activity toward APP and spare other substrates. A better understanding of the subcellular trafficking of γ-secretase complexes and their substrates may provide useful clues toward achieving this goal.

γ-Secretases are membrane-associated aspartyl proteases made of four core components (6–8), probably assembled in a 1:1:1:1 stoichiometry (7, 9, 10): the single pass transmembrane protein nicastrin (NCT) (11) and the multipass transmembrane proteins anterior pharynx-defective 1 (APH1a or APH1b) (12, 13), presenilin enhancer 2 (PEN2) (13), and presenilin (PS1 or PS2) (14, 15), which harbors the catalytic site of the enzyme (16). γ-Secretase assembly into a functional complex occurs in a stepwise manner in the endoplasmic reticulum (ER), where presenilin endoproteolysis (17) into N- and C-terminal fragments (NTF and CTF) is also achieved (18, 19). Important motifs responsible for ER retrieval/retention were evidenced in the transmembrane domains of PS1 (20), PEN2 (21), and NCT (22) and preclude trafficking of unassembled subunits beyond the ER. These signals are masked upon γ-secretase assembly (22, 23), allowing γ-secretase complexes to traffic further toward the Golgi apparatus, where NCT complex glycosylation is achieved (24, 25), and beyond. γ-Secretase complexes were indeed shown to be present and active toward APP and other substrates at various cellular sites, including the plasma membrane (26–30), endosomes (26, 31–35), and lysosomes (31, 36–38).

Importantly, as mentioned above, two homologues of PS (PS1 and PS2) and APH1 (APH1a and APH1b) were identified in humans, and their different combinations with other subunits can generate at least four distinct γ-secretase complexes. Moreover, alternatively spliced forms of PS (39) and APH1a (APH1aL and APH1aS) (40) were identified, increasing further

* This work was supported by the French National Foundation for Alzheimer Disease and Related Disorders (to X. M.) and by the European League against Alzheimer disease (LECMA) (to F. C.). This work has been developed and supported through the Hospital-University Federation (FHU Onco-Age) and the LABEX "Excellence Laboratory Program Investment for the Future" Development of Innovative Strategies for a Transdisciplinary Approach to Alzheimer disease (DISTALZ). The authors declare that they have no conflicts of interest with the contents of this article.

[S] This article contains supplemental Figs. S1 and S2 and Movies 1 and 2.

[1] To whom correspondence should be addressed: Institut de Pharmacologie Moléculaire et Cellulaire, CNRS UMR7275, 660 Route des Lucioles, 06560 Valbonne, France. Tel.: 334-93-95-34-60; Fax: 334-93-95-77-08; E-mail: checler@ipmc.cnrs.fr.

[2] The abbreviations used are: AD, Alzheimer disease; APP, amyloid precursor protein; Aβ, amyloid β; NCT, nicastrin; APH, anterior pharynx-defective; PEN, PS enhancer; PS, presenilin; ER, endoplasmic reticulum; CTF, C-terminal fragment; NTF, N-terminal fragment; BiFC, bimolecular fluorescence complementation; BACE, β-site APP-cleaving enzyme; AICD, APP intracellular domain; EGFP, enhanced GFP; FL, full-length; TGN, *trans*-Golgi network; DIV, days *in vitro*; Tricine, *N*,*N*-bis(2-hydroxyethyl)glycine (systematic); BisTris, 2-[bis(2-hydroxyethyl)amino]-2-(hydroxymethyl)propane-1,3-diol.

the theoretical diversity of γ-secretase complexes. The levels of expression of the variable subunits PS and APH1 can differ between tissues and/or cell types, but γ-secretase complexes of distinct composition can co-exist within the cell (41, 42). The influence of γ-secretase subunit variability on γ-secretase subcellular trafficking has not been fully explored, but it is worthy of attention because the targeting of a given γ-secretase complex to a specific cellular compartment may underlie the substrate specificity of this complex and thus yield useful information for designing more specific inhibitors of APP processing.

Recently, we used bigenic expression vectors to co-express the four γ-secretase subunits, including PS1 and different variants of APH1, and used bimolecular fluorescence complementation (BiFC) to visualize newly assembled γ-secretase complexes (36). We observed that PS1-containing γ-secretase complexes were mainly targeted to the plasma membrane and that those including APH1b were more retained/retrieved in the ER than those including APH1a.

In the present work, we generated new tools for the inducible, temporary, and stoichiometric expression of six different combinations of the four γ-secretase subunits. We show that these constructs allow the formation and maturation of functional γ-secretase complexes and their visualization in post-ER compartments. Remarkably, we observe distinct subcellular targeting of γ-secretase complexes depending on their presenilin subunits. PS1-containing γ-secretase complexes are targeted mainly to the plasma membrane, whereas PS2-containing ones are targeted to different types of endosomes, depending on their APH1 subunit. These results unravel the importance of γ-secretase composition for its cellular targeting. Our novel constructs should prove very useful to further explore the subcellular trafficking of γ-secretase complexes and to investigate the link between γ-secretase cellular compartmentalization and substrate specificity.

Experimental Procedures

Plasmid Constructs—All γ-secretase subunit cDNAs used here were of human origin. All of the constructs described here were verified by sequencing. The plasmid backbone for all of the constructs was pTRE3G-BI (Clontech), which harbors a doxycycline-inducible bidirectional promoter flanked by two multicloning sites. A BstBI site was introduced into pTRE3G-BI by cloning the following annealed primers into the BamHI and NotI sites: 5′-GATCCATCTTCGAAGATGC-3′ and 5′-GGCCGCATCTTCGAAGATG-3′. Transgene expression from pTRE3G-BI requires the co-transfection of pCMV-Tet3G (Clontech) for the expression of a transactivator protein that activates transcription from pTRE3G-BI promoter when bound to doxycycline.

The different inserts containing two γ-secretase subunits sequences separated by a 2A peptide sequence were designed according to Szymczak-Workman *et al.* (43). The C-terminally EGFP-tagged nicastrin sequence was PCR-amplified from pEGFP-N1-nicastrin (36) using the following primers in order to introduce the 2A peptide sequence from porcine teschovirus-1 (P2A, ATNFSLLKQAGDVEENPGP) downstream of nicastrin-EGFP sequence: 5′-CGCTCTTTCGAAGCCACCATGGCTACGGCAG-3′ and 5′-CAGCCTGCTTCAGCAGGCTGAAGTTAGTAGCTCCGGATCCCTTGTACAGCTCGTCCATGC-3′. The PEN2 sequence was PCR-amplified using pCDNA4-PEN2-myc-His (44) as a template and the following primers to introduce the P2A peptide sequence upstream of the PEN2 sequence: 5′-CAGCCTGCTGAAGCAGGCTGGAGACGTGGAGGAGAACCCTGGACCTATGAACCTGGAGCGAGTGTC-3′ and 5′-CCGACAGCGGCCGCCTAGGGGGTGCCCAGGG- 3′. The resulting nicastrin-EGFP-P2A and P2A-PEN2 PCR products were combined as template and PCR-amplified using the external primers specific for the 5′-end of nicastrin and the 3′-end of PEN2 sequences. The resulting nicastrin-EGFP-P2A-PEN2 PCR product was digested by BstBI/NotI and subcloned into the first multicloning site of pTRE3G-BI-BstBI to create pTRE3G-BI-1-NCT-EGFP-P2A-PEN2.

The different APH1 variant sequences were PCR-amplified using pEGFP-C1-APH1 constructs (36) as templates and the following primers in order to introduce the 2A peptide sequence from *Thosea asigna* virus (T2A, EGRGSLLTCGDVEENPGP) downstream of APH1 variant sequences: 5′-CGCTCTACGCGTGCCACCATGGGGGCTGCGGTGTTTTTC-3′ and 5′-CACGTGAGCAGACTTCCTCTGCCCTCTCCCGAACCGTCCTCGGGTGGGATGCG-3′ (APH1aL) or 5′-CACGTGAGCAGACTTCCTCTGCCCTCTCCCGAACCGTCCTTGCACAAGAGGCTGC-3′ (APH1aS); 5′-CGCTCTACGCGTGCCACCATGACTGCGGCCGTGTTCTTC-3′ and 5′-CACGTGAGCAGACTTCCTCTGCCCTCTCCCGAACCTCTGGAGCGCTGGTTGTAAAG-3′ (APH1b). The PS1 sequence was PCR-amplified using a pCDNA3-PS1-WT construct, generated previously in our laboratory from a human kidney cDNA library (45), as a template and the following primer set to introduce the T2A peptide sequence upstream of the PS1 sequence: 5′-GCAGAGGAAGTCTGCTCACGTGCGGTGACGTCGAGGAGAATCCTGGCCCAATGACAGAGTTACCTGCACCG-3′/5′-GGGCCCTCTAGACTAGATATAAAATTG-3′. The PS2 sequence was PCR-amplified using a pCDNA3-PS2-WT construct (46), where PS2 cDNA comes from reverse transcribed adult human brain RNA (17), as a template and the following primer set to introduce the T2A peptide sequence upstream of the PS2 sequence: 5′-GCAGAGGAAGTCTGCTCACGTGCGGTGACGTCGAGGAGAATCCTGGCCCAATGCTCACATTCATGGCCTCTG-3′/5′-CCCTCTAGACCTCAGATGTAGAG-3′. The resulting APH1aL-T2A or APH1aS-T2A or APH1b-T2A and T2A-PS1 or T2A-PS2 PCR products were combined pairwise as template and PCR-amplified using the external primers specific for the 5′-end of APH1a or APH1b and the 3′-end of PS1 or PS2 sequences. The resulting APH1(aL or aS or b)-T2A-PS(1 or 2) PCR products were digested by MluI/XbaI and subcloned into the second multicloning site of pTRE3G-BI-1-NCT-EGFP-P2A-PEN2 to create pTRE3G-BI-1-NCT-EGFP-P2A-PEN2_2-APH1aL-T2A-PS1, pTRE3G-BI-1-NCT-EGFP-P2A-PEN2_2-APH1aS-T2A-PS1, pTRE3G-BI-1-NCT-EGFP-P2A-PEN2_2-APH1b-T2A-PS1, pTRE3G-BI-1-NCT-EGFP-P2A-PEN2_2-APH1aL-T2A-PS2, pTRE3G-BI-1-NCT-EGFP-P2A-PEN2_2-APH1aS-T2A-PS2, and pTRE3G-BI-1-NCT-EGFP-P2A-PEN2_2-APH1b-T2A-PS2 (Fig. 1*A*).

APH1aL sequence was PCR-amplified using pEGFP-C1-APH1 as a template and the following primer set: 5′-CGCTC-

TACGCGTGCCACCATGGGGGCTGCGGTGTTTTTC-3′/5′-CGCTCTTCTAGATTAGTCCTCGGGTGGGATGCG-3′. PS1 sequence was PCR-amplified using pCDNA3-PS1-WT as a template and the following primer set: 5′-CGCTCTACGCGTGCCACCATGACAGAGTTACCTG-3′/5′-GGGCCCTCTAGACTAGATATAAAATTG-3′. The resulting PCR products were digested by MluI/XbaI and subcloned into the second multicloning site of pTRE3G-BI-1-NCT-EGFP-P2A-PEN2 to create pTRE3G-BI-1-NCT-EGFP-P2A-PEN2_APH1aL and pTRE3G-BI-1-NCT-EGFP-P2A-PEN2_2-PS1 (Fig. 1*B*). The C-terminally EGFP-tagged nicastrin sequence was PCR-amplified from pEGFP-N1-nicastrin using the following primer set: 5′-CGCTCTTTCGAAGCCACCATGGCTACGGCAG-3′/5′-GTCGCGGCCGCTTTACTTG-3′. The resulting PCR product was digested by BstBI/NotI and subcloned into pTRE3G-BI-1-NCT-EGFP-P2A-PEN2_2-APH1aL-T2A-PS1 to create pTRE3G-BI-1-NCT-EGFP_2-APH1aL-T2A-PS1 (Fig. 1*B*).

Cell Culture, Transfections, and Induction Protocols for Biochemical Analyses—COS-7 cells (ECACC) were plated in 100-mm dishes at a density of 3×10^4 cells/cm^2 in Dulbecco's modified Eagle's medium (Gibco) supplemented with 10% FBS (Sigma). Eighteen hours after plating, cells were co-transfected with 2.4 μg of pCMV-Tet3G- and 9.6 μg of pTRE3G-BI-based constructs (see above and Fig. 1) per 100-mm dish, using jetPRIME transfection reagent according to the manufacturer's instructions (Polyplus transfection). Twenty-two hours after transfection, transgene expression was induced transiently for 5 h with 1 μg/ml doxycycline in culture medium and then stopped with three washes in 1× PBS before placing the cells back in culture medium. Nineteen hours after induction, cells were processed to prepare membrane-enriched fractions or lysed for co-immunoprecipitation experiments (see below).

HEK293 cells stably expressing APP_{WT} and β-site APP-cleaving enzyme 1 (BACE1) (47) were plated in a poly-L-lysine-coated (0.05 mg/ml) 6-well plate at a density of 1×10^5 cells/cm^2 in Dulbecco's modified Eagle's medium supplemented with 10% FBS, G418 (600 μg/ml), and zeocin (200 μg/ml). Eighteen hours after plating, cells were co-transfected with 0.4 μg of pCMV-Tet3G- and 1.6 μg of pTRE3G-BI-based constructs per well, using jetPRIME transfection reagent. Seven hours after transfection, transgene expression was induced transiently for 15 h with 0.5 μg/ml doxycycline in culture medium and then stopped with two washes in 1× PBS before placing the cells back in culture medium. Eight hours after induction, cells were placed in secretion medium (Opti-MEM I (Gibco) supplemented with 1% FBS). After 16 h, secretion medium was collected and supplemented with protease inhibitor mixture (Sigma, 1× final), and cells were scraped in lysis buffer (150 mM NaCl, 50 mM Tris-HCl, pH 7.4, 0.5% Igepal CA630, 0.5% sodium deoxycholate, 5 mM EDTA, 0/25% SDS, 1× Sigma protease inhibitor mixture) and sonicated for 30 s on ice.

Preparation of Membrane-enriched Fractions and in Vitro γ-Secretase Assay—Membrane-enriched fractions were prepared mainly as described previously (48) and used for an *in vitro* γ-secretase assay (49). The production of γ-secretase metabolites was analyzed by Western blotting using 16.5% Tris-Tricine gels and a combination of mouse monoclonal anti-FLAG M2 (F1804, Sigma) and anti-Aβ(1–12) 2H3 (50) antibodies (kind gift of Dr. D. Schenk, Elan Biosciences, South San Francisco, CA) to visualize APP intracellular domain (AICD) and Aβ, respectively. The peak heights of signal intensities from AICD and Aβ bands were quantified with ImageJ software using the central third of the lane width for analysis according to Gassmann *et al.* (51).

Co-immunoprecipitation—Co-immunoprecipitation of γ-secretase subunits with EGFP-tagged nicastrin (NCT-EGFP) was performed as described previously (36). NCT-EGFP was immunoprecipitated using 800 μg of total proteins solubilized with CHAPSO buffer (1% CHAPSO, 150 mM NaCl, 50 mM HEPES, pH 7.4, 2 μM EDTA, protease inhibitor mixture) from COS-7 cells (see above) and 2.5 μl of mouse monoclonal anti-GFP antibodies (Roche Applied Science, mixture of clones 7.1 and 13.2).

Western Blotting—Membrane fractions, cell lysates (50 μg of total proteins; see below), or co-immunoprecipitated proteins were separated on 7% (nicastrin), 12% (APH1s, presenilins) polyacrylamide Tris-glycine gels, or 16.5% polyacrylamide Tris-Tricine gels (PEN2), followed by transfer onto PVDF membranes (Bio-Rad). The following rabbit polyclonal antibodies were used: anti-2A peptide raised against the 2A peptide sequence derived from foot and mouth picornavirus (ABS31, Merck Millipore); anti-APH1aL raised against the C-terminal region of human APH1aL (kind gift from Dr. St George-Hyslop) (40); anti-PEN2 raised against the last 24 amino acids of human PEN2 (CR8, Covance); anti-$PS1_{NT}$ raised against residues 1–65 of human PS1 (52); and anti-$PS2_{loop}$ raised against residues 269–394 from the intracellular loop region of human PS2 (17). The rabbit monoclonal anti-PEN2 raised against the N-terminal part of PEN2 was used only in Fig. 4 (D2G6, Cell Signaling Technology). Nicastrin was detected using a goat polyclonal antibody raised against the N terminus of human nicastrin (sc-14369, Santa Cruz Biotechnology, Inc.). EGFP-tagged nicastrin was revealed using mouse monoclonal anti-GFP antibodies (Roche Applied Science, mixture of clones 7.1 and 13.2). Proteins were visualized using enhanced chemiluminescence (SuperSignal West Pico or Femto, Thermo Scientific) and acquired with a cooled CCD camera from an LAS-4000 imaging system (Fujifilm).

Preparation and Separation of Native γ-Secretase Complexes—Membrane-enriched fraction pellets from COS-7 cells (see above) were resuspended in 60 μl of 1× NativePAGE sample buffer (Invitrogen), 1% digitonin, 1× protease inhibitor mixture (Sigma), followed by a 25-min incubation on ice. Insoluble material was pelleted (100,000 × *g*, 20 min at 4 °C), and the supernatants corresponding to solubilized proteins were collected. Thirteen micrograms of solubilized proteins were separated at 6 °C using the NativePAGE Novex BisTris 3–12% polyacrylamide gradient gel system from Invitrogen according to the manufacturer's recommendations, which is based on the blue native PAGE technique developed by Schägger and von Jagow (53). NativeMark unstained protein standard (Invitrogen) was used for molecular weight estimation. Following blue native PAGE, proteins were transferred onto a PVDF membrane in NuPAGE transfer buffer (Invitrogen). The membrane was then incubated in 8% acetic acid for 15 min, rinsed

in deionized water, and air-dried. The membrane was rewet in methanol prior to immunodetection with anti-GFP antibodies (described above).

ELISA Quantification of Aβ Peptides—The secreted medium collected from transfected HEK293 APP_{WT}/BACE1 stable cells (see transfection and induction protocols above) was diluted 1:40 for Aβ40 analysis and 1:3 for Aβ42 analysis using specific ELISA kits from Invitrogen.

Fluorescence Microscopy—COS-7 cells were plated on 18-mm acid-washed coverslips in 12-well plates for immunocytochemistry experiments or on 25-mm acid-washed coverslips in 6-well plates for live imaging at a density of 7.5×10^3 cells/cm^2. Cells were co-transfected 16 h after plating with 0.2 μg of pCMV-Tet3G and 0.8 μg of pTRE3G-BI constructs (see "Plasmid Constructs") per well (for 12-well plates or twice these amounts for 6-well plates) using jetPRIME transfection reagent (Polyplus transfection). Twenty-two hours after transfection, transgene expression was induced transiently for 2 h with 1 μg/ml doxycycline.

For immunocytochemistry, 22 h after induction, cells were fixed for 20 min in paraformaldehyde (4%) and sucrose (4%) in PBS. Free aldehyde groups were quenched by incubation in glycine (100 mM in PBS) for 10 min. Cells were then permeabilized with Triton X-100 (0.2%), BSA (3% in PBS) for 5 min at room temperature, followed by an additional blocking step in BSA (3% in PBS) for 30 min. Primary and secondary antibodies were diluted in BSA (0.3% in PBS) and incubated successively (45 min each). Coverslips were mounted in a Mowiol medium containing 1,4-diazabicyclo-[2,2,2]-octane (DABCO; 2.5%), (26, 54). The following primary antibodies were used: goat polyclonal anti-calreticulin (sc-6467, Santa Cruz Biotechnology); mouse monoclonal anti-EEA1 (clone 14/EEA1, catalog no. 610457, BD Biosciences), anti-CD71/transferrin receptor (ascites fluid, clone H68.4), and anti-CD63 (ab23792, Abcam); and sheep polyclonal anti-TGN46 (AHP500G, AbD Serotec). Alexa Fluor 594-conjugated donkey anti-goat, anti-mouse, or anti-sheep secondary antibodies (Molecular Probes) were used. Images were acquired using a confocal scanning inverted microscope (LSM780, Zeiss) controlled by ZEN software (Zeiss) or an inverted wide field fluorescence microscope (Axiovert 200M, Zeiss) controlled by Metamorph version 6.1 software (Molecular Devices) equipped with a cooled charge-coupled device (CCD) camera (Coolsnap HQ, Photometrics) using ×63/numerical aperture 1.4 Plan Apochromat oil objectives (Zeiss). For labeling of endo/lysosomes, cells were incubated with LysoTracker Red DND-99 (50 nM; Molecular Probes) in culture medium for 30 min at 37 °C and then washed three times with PBS prior to fixation. Images were processed using ImageJ software (27). To improve the visualization of the vesicular staining of γ-secretase complexes containing PS2 or the reticular stainings (Fig. 2*B*), images were processed with an unsharpmask filter.

For live imaging experiments, time lapse images were captured with a spinning disk confocal unit (CSUX1-A3, Yokogawa) on an inverted microscope (Eclipse Ti-E, Nikon) equipped with a Perfect Focus system (Nikon), an electron multiplying charge-coupled device camera (C9100-50, Hamamatsu), and Volocity version 6.0.1 acquisition software (PerkinElmer Life Sciences), using a ×60/numerical aperture 1.4 CFI Plan Apochromat oil objective (Nikon). Transfected COS-7 cells were imaged inside a 37 °C incubation chamber filled with a Hepes-buffered saline solution (140 mM NaCl, 2.5 mM KCl, 1.8 mM $CaCl_2$, 1 mM $MgCl_2$, 5 mM glucose, 20 mM Hepes, pH 7.4).

Primary Neuronal Cultures and Transfections—The following experimental procedures were in accordance with the European Communities Council Directive of 24 November 1986 (86/609/EEC) and local French legislation. Hippocampal neurons were prepared from Sprague-Dawley rat embryos (*Rattus norvegicus*, RjHan:SD strain, mixed male and female day 18 embryos, Janvier Labs) according to Kaech and Banker (26), plated at a density of 12,500 cells/cm^2 on poly-D-lysine-coated (0.1 mg/ml, 70,000–150,000 g/mol polymers; Sigma) glass coverslips (Menzel Gläser) equipped with paraffin dots, and cultured in Neurobasal medium supplemented with B27 (both from Gibco) and 1-β-D-arabinofuranosylcytosine (5 μM; Sigma), facing a glial feeding layer grown on 60-mm dishes. Glial cells were prepared from the cortex of Sprague-Dawley rat embryos (embryonic day 18) 2 weeks before the neuronal culture according to Zeitelhofer *et al.* (31). Cultured neurons were transfected at 6 days *in vitro* (DIV) using Lipofectamine 2000 (5 μl; Invitrogen), 0.6 μg of pCMV-Tet3G, and 2.4 μg of pTRE3G-BI constructs diluted in a final volume of 200 μl of Opti-MEM medium (Gibco) for each 60-mm dish. Transgene expression was induced at 16 DIV with doxycycline (500 ng/ml) for 5 h. Neurons were fixed at 17 DIV, and coverslips were mounted using the same procedure as for COS-7 cells (see above).

Statistical Analysis—Statistical analyses were performed with Prism version 4 (GraphPad Software) using repeated measure one-way analysis of variance followed by Newman-Keuls multiple comparison tests.

Results

Generation of New Tools for the Inducible, Temporary, and Stoichiometric Co-expression of Four γ-Secretase Subunits and the Visualization of Assembled γ-Secretase Complexes—Our previous work with BiFC constructs (36) showed us that a continuous expression of γ-secretase subunits leads to the accumulation of unassembled or preassembled γ-secretase subunits within the ER that can obscure the visualization of mature γ-secretase complexes in post-ER compartments. To avoid this drawback, we chose to express given sets of γ-secretase subunits using a commercial vector containing a bidirectional and doxycycline-inducible promoter (Fig. 1*A*), allowing a temporary and equimolar co-expression of two transgenes. By stopping the induction, we should allow γ-secretase complex maturation and trafficking away from the ER to their cellular destination(s) before their examination.

We also aimed at favoring a stoichiometric expression of the four γ-secretase subunits; therefore, we could not rely on the co-transfection of two vectors with bidirectional promoters. To achieve this goal, we took advantage of the 2A peptide-linked multicistronic vector technology, which allows the expression of multiple proteins from a single open reading frame (43). The "self-cleaving" 2A peptide sequence was initially characterized

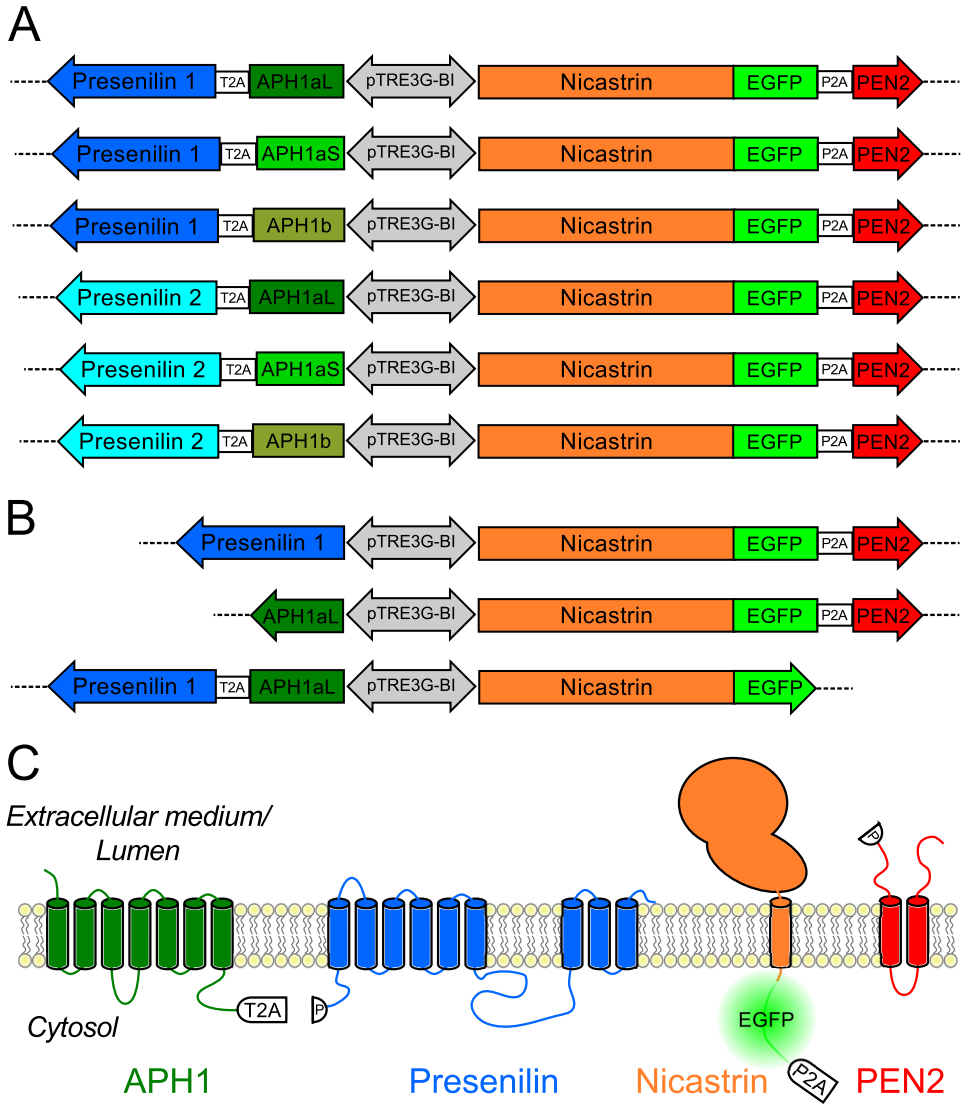

FIGURE 1. **Novel vectors for the stoichiometric and inducible expression of the different combinations of γ-secretase subunits and their visualization.** *A*, schematics of the plasmid constructs generated to express six different combinations of the four γ-secretase subunits varying by their presenilin (1 or 2) and APH1 (aL, aS, or b) subunits. The pTRE3G-BI promoter (*gray bidirectional arrow*) allows for simultaneous, equivalent, and inducible expression of the two transgenes cloned beside it. The 2A peptide sequences (T2A and P2A, white boxes) cloned between two genes, allow for equivalent production of two discrete proteins through a "cleavage" event within the 2A peptide sequence (43). Nicastrin was C-terminally tagged with EGFP separated by a 10-amino acid flexible linker. These constructs are referred to as follows (from *top* to *bottom*): 4γ-PS1/APH1aL, 4γ-PS1/APH1aS, 4γ-PS1/APH1b, 4γ-PS2/APH1aL, 4γ-PS2/APH1aS, and 4γ-PS2/APH1b. *B*, schematics of the control plasmid constructs generated to co-express only three γ-secretase subunits together. These constructs are referred to as follows (the missing subunit is indicated in parentheses): 3γ-(−APH1), 3γ-(−PS1), and 3γ-(−PEN2). *C*, schematics of the γ-secretase subunits synthesized from 4γ-PS/APH1 constructs indicating the positions of 2A and EGFP tags. The proline residue remaining after the 2A-peptide "cleavage," at the N terminus of the γ-secretase subunits placed downstream of 2A sequences, is indicated (*P*).

in foot and mouth picornavirus (55), and since then, many other 2A peptide sequences have been identified in other viruses and some parasites. The 2A peptide "cleavage" actually occurs through a ribosomal skip mechanism at the end of 2A peptide sequences (56). These sequences can be placed between genes within a single vector to allow stoichiometric production of discrete protein products. Because the "cleavage" occurs at the end of the 2A sequence, most of the peptide (<20 amino acids) will consequently remain attached to the protein placed upstream of the 2A peptide. This was an important aspect to consider for choosing the position at which to clone γ-secretase subunit sequences around a 2A peptide sequence. We chose to subclone the C-terminal EGFP-tagged nicastrin (NCT-EGFP) and PEN2 sequences separated by the P2A peptide (see "Experimental Procedures") on one side of the bidirectional promoter (Fig. 1*A*) because PEN2 is destabilized by C-terminal tags that interfere with interactions with other γ-secretase components (44), whereas nicastrin was successfully tagged at its C terminus without affecting interactions with other γ-secretase components (11, 57–59). We subcloned the different combinations of APH1 (APH1aL, APH1aS, or APH1b) and presenilin (PS1 or PS2) sequences separated by the T2A sequence on the other side of the bidirectional promoter (Fig. 1*A*), because the C terminus of PS1 is required for γ-secretase assembly and activity (20, 60) and could be perturbed by a tag, whereas APH1 was C-terminally tagged without noticeable effect on APH1 interaction with other γ-secretase subunits or γ-secretase assembly (7, 61). Overall, the combination of the bidirectional promoter

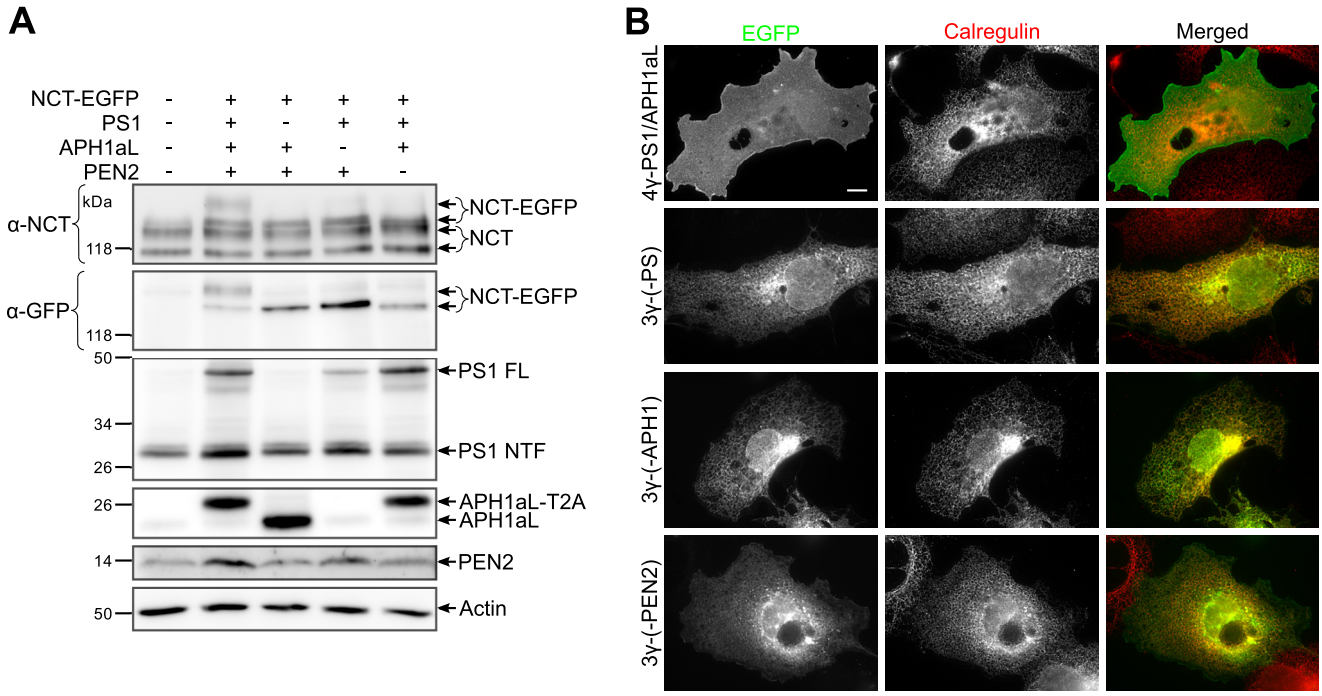

FIGURE 2. **The temporary co-expression of four γ-secretase subunits allows their maturation and visualization outside the ER.** *A*, COS-7 cells were co-transfected with the following (from *lane 1* to *lane 5*): empty vector, 4γ-PS1/APH1aL, 3γ-(−APH1), 3γ-(−PS1), or 3γ-(−PEN2) and the transactivator-protein expression plasmid. Transgene expression was induced with doxycycline for 5 h the next day, and cells were lysed 20 h after induction and analyzed by Western blot using specific antibodies for each γ-secretase subunit or an anti-GFP antibody to discriminate NCT-EGFP from endogenous NCT. *B*, COS-7 cells were co-transfected with the constructs indicated on the *left* and the transactivator-protein expression plasmid; transgene expression was induced with doxycycline for 2 h the next day, and cells were fixed 22 h after induction, processed for immunocytochemistry to label the ER marker calregulin, and analyzed using wide field epifluorescence microscopy. *Scale bar*, 10 μm.

and 2A peptide technology should achieve the synthesis of discrete γ-secretase subunits, including T2A-tagged APH1 and EGFP-P2A-tagged nicastrin (Fig. 1*C*). For better clarity, we will refer hereafter to these constructs as "4γ-PS/APH1," because they allow the co-expression of the four γ-secretase subunits (4γ) and to indicate the six specific combinations of the variable subunits PS and APH1, namely 4γ-PS1/APH1aL, 4γ-PS1/APH1aS, 4γ-PS1/APH1b, 4γ-PS2/APH1aL, 4γ-PS2/APH1aS, or 4γ-PS2/APH1b.

We decided to tag nicastrin with EGFP as a reporter of γ-secretase localization, because it is a component common to all γ-secretase complexes. Our previous experiments using BiFC constructs showed us that no signal from fluorescently tagged γ-secretase subunits can be detected in post-ER compartments without the co-transfection of the four γ-secretase subunits and the formation of new γ-secretase complexes (36). We therefore assumed that with the above-described new constructs, the fluorescence derived from EGFP-tagged nicastrin in post-ER compartments would genuinely reflect γ-secretase localization and not only nicastrin localization. However, to confirm this postulate, we generated control constructs in which only three γ-secretase subunits will be co-expressed (Fig. 1*B*) that we will refer to as "3γ" followed by the missing subunit: 3γ-(−APH1), 3γ-(−PS), or 3γ-(−PEN2). Overall, our new vectors are the first constructs permitting inducible and temporary stoichiometric expressions of all γ-secretase subunit combinations and should allow the visualization of specific γ-secretase complexes in the cell to assess the putative differences in their subcellular localization and trafficking.

The Co-induced Temporary Expression of the Four γ-Secretase Subunits Is Required and Sufficient for the Maturation of Newly Formed γ-Secretase Complexes and Their Detection Outside the ER—To validate our strategy to visualize mature γ-secretase complexes in the cell only through the detection of NCT-EGFP, we first compared the expression of γ-secretase subunits in COS-7 cells transfected with 4γ-PS1/APH1aL or its control constructs (Fig. 2*A*). In 4γ-PS1/APH1aL-transfected cells, we observed an increased intensity of the bands corresponding to PS1-NTF or PEN2 as compared with empty vector-transfected cells and the appearance of new bands for NCT-EGFP-P2A and APH1-T2A at their expected molecular weights, slightly over endogenous subunits, showing that the 2A peptide "cleavages" occurred efficiently and that our 4γ-PS1/APH1aL construct achieved the expression of discrete γ-secretase subunits. Using an anti-GFP antibody to detect transgenic NCT-EGFP, we observed a band doublet only for the cells transfected with 4γ-PS1/APH1aL, whereas cells transfected with all control "3γ" constructs presented only the lower band with a higher intensity. The upper band of the doublet appeared thicker and more intense than the lower one and probably corresponded to mature glycosylated NCT-EGFP. Indeed, nicastrin complex glycosylation requires its exit from the ER and trafficking through the Golgi apparatus, and γ-secretase complex assembly is necessary for ER exit (22). In 4γ-PS1/APH1aL-transfected cells, full-length PS1 (PS1 FL) was still detectable (Fig. 2*A*); however, a clear increase of endoproteolyzed PS1 N-terminal fragment (PS1 NTF), as compared with empty vector-transfected cells, was also observed. This

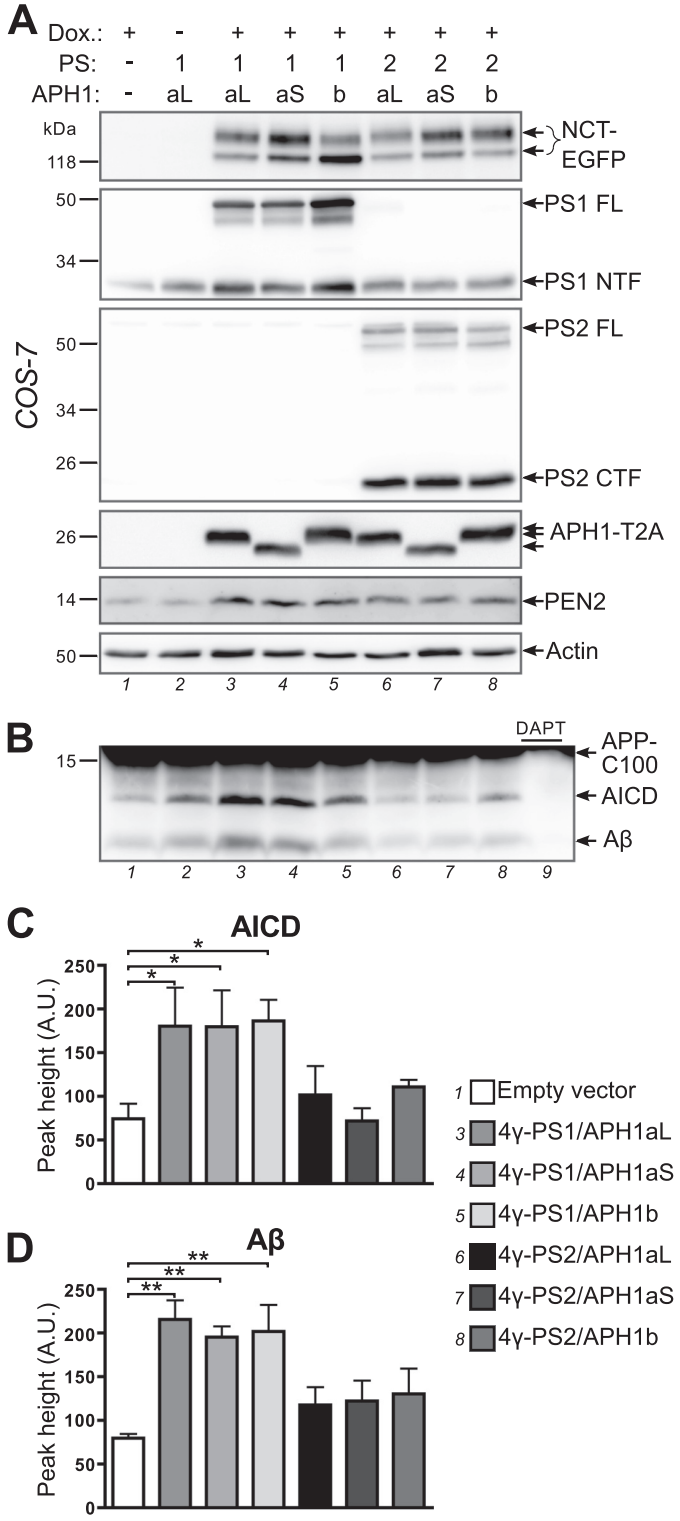

FIGURE 3. **Expression of distinct and functionally active γ-secretase complexes.** *A*, COS-7 cells were co-transfected with empty vector (*lane 1*), 4γ-PS1/APH1aL (*lanes 2* and *3*), 4γ-PS1/APH1aS, 4γ-PS1/APH1b, 4γ-PS2/APH1aL, 4γ-PS2/APH1aS, or 4γ-PS2/APH1b (*lanes 4–8*), and the transactivator protein expression plasmid; transgene expression was induced or not with doxycycline (*Dox.*) for 5 h the next day, and cells were processed to recover a membrane-enriched fraction 1 day after induction and analyzed by Western blot using specific antibodies for each γ-secretase subunit or an anti-GFP antibody to detect NCT-EGFP and an anti-2A peptide antibody to detect APH1-T2A. *B*, membrane-enriched fractions analyzed in *A* were used for a γ-secretase *in vitro* activity assay using an APP-C100-FLAG substrate. The production of AICD-FLAG and Aβ was analyzed by Western blot using a combination of anti-FLAG and anti-Aβ antibodies. In *lane 9*, the γ-secretase inhibitor *N*-[*N*-(3,5-difluorophenacetyl)-L-alanyl]-*S*-phenylglycine *t*-butyl ester was added to the reaction using the membrane fraction corresponding to *lane 3* (4γ-PS1/APH1aL). *C* and *D*, quantification of AICD-FLAG (*C*) and Aβ (*D*) production in γ-secretase *in vitro* assays. *A.U.*, arbitrary units. Results are presented as mean ± S.E. (*error bars*) ($n = 4$). Statistical analysis using repeated measures analysis of variance revealed that means for AICD-FLAG and Aβ were significantly different ($p < 0.01$); Newman-Keuls multiple-comparison tests revealed significant differences between cells transfected with empty vector control and the ones transfected with PS1-containing vectors (*, $p < 0.05$; **, $p < 0.01$). The full results of Newman-Keuls pairwise comparisons are presented in Table 1.

observation was an additional proof of efficient maturation of γ-secretase complexes in 4γ-PS1/APH1aL-transfected cells as PS1 endoproteolysis occurs during γ-secretase assembly.

We next analyzed NCT-EGFP fluorescence in COS-7 cells transfected with 4γ-PS1/APH1aL or its control "3γ" constructs, for which transgene expression was transiently induced 22 h before fixation and microscope observation to allow newly synthesized γ-secretase complex maturation and trafficking to their cellular destinations. Cells transfected with "3γ" constructs displayed an EGFP fluorescence restricted to the ER, particularly intense around the nucleus, overlapping with the ER marker calregulin (Fig. 2*B*). Conversely, in 4γ-PS1/APH1aL-transfected cells, NCT-EGFP fluorescence did not overlap with calregulin staining. In particular, the nuclear envelope, which is contiguous to the ER and clearly visible in control cells, was barely detectable. In these cells, NCT-EGFP fluorescence was mainly detected at the plasma membrane, highlighting the cell edges. These results, together with the observation of a combined NCT-EGFP glycosylation and PS1 endoproteolysis only in 4γ-PS1/APH1aL-transfected cells (Fig. 2*A*), demonstrate that the NCT-EGFP detected at the plasma membrane was genuinely associated with mature γ-secretase complexes and truly reflected the localization of newly assembled γ-secretase complexes (*i.e.* containing PS1 and APH1aL).

γ-Secretase Subunit Compositions Drive Distinct Levels of Maturation into Functional γ-Secretase Complexes—We next analyzed the expression of γ-secretase subunits in membrane-enriched fractions prepared from COS-7 cells transfected with the different 4γ-PS/APH1 constructs (Fig. 3*A*). We detected a band doublet for NCT-EGFP, presenting a more intense mature upper band except for the cells transfected with 4γ-PS1/APH1b, for which the immature band appeared more prominent. This observation reflects a slower maturation of PS1- and APH1b-containing γ-secretase complexes and could indicate a higher degree of ER retention/retrieval of these γ-secretase complexes. This difference was clearly linked to the nature of the PS because the NCT-EGFP mature band was similarly prevalent in all 4γ-PS2/APH1-transfected cells.

Full-length PS1 or PS2 was still detectable 20 h after the end of induction, in all 4γ-PS/APH1-transfected cells, concomitant with a clear increase in PS1 NTF or PS2 CTF immunoreactivities (as compared with empty vector control or non-induced cells (Fig. 3*A*, *lanes 1* and *2*)), indicating the assembly and maturation of new γ-secretase complexes in 4γ-PS/APH1-transfected cells. However, despite comparable levels of expression of PEN2 and APH1-T2A between all of the 4γ-PS/APH1-transfected cells, obvious differences were observed in the PS1 NTF/

PS1 FL and PS2 CTF/PS2 FL ratios, indicating the following. First, PS endoproteolysis was more efficient for PS2-containing γ-secretase complexes than for those harboring PS1; second, the extent of PS1 endoproteolysis varied according to the nature of the APH1 isoform, with APH1b leading to a lower extent of maturation. This slower PS1 endoproteolysis of PS1/APH1b-containing γ-secretase complexes agreed well with their lower degree of nicastrin glycosylation.

To assess the functionality of newly formed γ-secretase complexes, we used the membrane fractions characterized above to perform γ-secretase *in vitro* activity assays (49), and we analyzed the production of AICD and Aβ (Fig. 3*B*). We did not detect any transfected subunit expression in non-induced cells. However, we chose to use empty vector-transfected cells as a control, because they went through the exact same treatments. AICD production was significantly increased in COS-7 cells transfected with PS1-containing constructs (Fig. 3*C*; empty vector, 74 ± 17; 4γ-PS1/APH1aL, 180 ± 44; 4γ-PS1/APH1aS, 180 ± 42; 4γ-PS1/APH1b, 186 ± 24), whereas cells transfected with PS2-containing constructs yielded AICD amounts comparable with empty vector-transfected cells (4γ-PS2/APH1aL, 102 ± 33; 4γ-PS2/APH1aS, 72 ± 15; 4γ-PS2/APH1b, 111 ± 8). Similarly, Aβ production was significantly increased in the cells transfected with PS1-containing constructs (Fig. 3*C*; empty vector, 80 ± 5; 4γ-PS1/APH1aL, 215 ± 22; 4γ-PS1/APH1aS, 195 ± 12; 4γ-PS1/APH1b, 202 ± 31), whereas expressions of PS2-containing complexes triggered only slightly higher Aβ productions (4γ-PS2/APH1aL, 117 ± 21; 4γ-PS2/APH1aS, 122 ± 23; 4γ-PS2/APH1b, 130 ± 29).

This significant increase of γ-secretase *in vitro* activity over endogenous activity observed in COS-7 cells transfected with PS1-containing constructs demonstrates that the GFP-P2A tag attached to transgenic nicastrin or the T2A tag attached to transgenic APH1s did not alter γ-secretase activity of the new γ-secretase complexes made from 4γ-PS1/APH1 constructs. These results are in agreement with the original results showing that the co-expression of the four core components of γ-secretase is sufficient to increase γ-secretase *in vitro* activity in mammalian cells (7, 8, 62). The absence of significant increases in AICD and Aβ productions in the cells transfected with 4γ-PS2/APH1 constructs is in accordance with the reported lower *in vitro* activity toward APP-based substrates of PS2-containing γ-secretase complexes as compared with PS1-containing ones (59, 63, 64).

Assembly and Distinct Maturation of the Four γ-Secretase Subunits into High Molecular Weight γ-Secretase Complexes—The concomitant glycosylation of NCT-EGFP and increased endoproteolysis of presenilins observed only when the four γ-secretase subunits were co-expressed, as well as the increased γ-secretase activity measured with the transfection of 4γ-PS1/APH1 constructs, suggested the formation of new γ-secretase complexes but did not prove directly the interaction of newly synthesized subunits into a complex. To confirm this hypothesis, we performed co-immunoprecipitation experiments, using an anti-GFP antibody to immunoprecipitate NCT-EGFP (Fig. 4, *A* and *B*). APH1-T2A, PEN2, and full-length and endoproteolyzed fragments of PS1 (Fig. 4*A*) or PS2 (Fig. 4*B*) were co-immunoprecipitated with both mature and immature NCT-EGFP. These observations demonstrate the interaction and assembly of transfected γ-secretase subunits into genuine *de novo* γ-secretase complexes. This also confirmed the presence of both mature γ-secretase complexes (containing fully glycosylated NCT-EGFP and endoproteolyzed PS) and immature complexes (made of immature NCT-EGFP and full-length PS) in transiently induced cells, the latter ones being more abundant in 4γ-PS1/APH1-transfected cells.

Next, to determine whether γ-secretase subunits expressed from 4γ-PS/APH1 constructs assembled into high molecular weight complexes and, thus, behave as their endogenous counterparts, we solubilized native γ-secretase complexes from membrane-enriched fractions in 1% digitonin buffer and performed blue native PAGE followed by Western blotting using an anti-GFP antibody to identify the protein complexes where NCT-EGFP was incorporated (Fig. 4*C*). A major immunoreactive band was observed above the 480 kDa marker (high molecular mass band) for all cells transfected with the different 4γ-PS/APH1 constructs and appeared to be the only band for PS2-containing γ-secretase complexes. Considering the additional mass brought by EGFP and 2A peptide tags (~30 kDa), this major band agrees well with the expected mass described for endogenous γ-secretase complexes (~440 kDa) by several groups using this technique and 1% digitonin solubilization (42, 65). Additional bands were detected for PS1-containing γ-secretase complexes. The major one appeared just below the 480 kDa marker (lower molecular mass band) and was as intense as the high molecular mass band for APH1b-containing complexes but slightly less intense for APH1aL- or APH1aS- and PS1-containing γ-secretases. The presence and the intensity of this lower molecular mass band clearly correlate with the lower levels of PS endoproteolysis and NCT-EGFP maturation specifically observed with PS1-containing complexes (Fig. 3*A*). Importantly, we did not detect any signal in the vicinity or below the 146 kDa marker, showing that 24 h after the end of the induction, all of the NCT-EGFP that was synthesized was either incorporated into higher molecular weight complexes or degraded. This observation further strengthens our interpretation that mature and immature γ-secretase complexes co-exist at this time point and that even the immature NCT-EGFP is probably incorporated in partially assembled or immature γ-secretase complexes.

Distinct γ-Secretase Subunit Combinations Differently Affect Aβ Peptides Secretion—In γ-secretase *in vitro* assays, γ-secretase complexes and a recombinant APP substrate are brought together in a reconstituted membrane environment. Therefore, a specific γ-secretase complex with a given PS/APH1 combination could have processed an APP substrate that it does not physiologically encounter within the cell because of distinct cellular targeting of this particular complex and APP β-CTF. To determine whether γ-secretase complexes assembled from our 4γ-PS/APH1 constructs can differently contribute to the processing of β-CTFs in a more integrated system, we analyzed Aβ40 and Aβ42 cellular secretions from HEK293 cells stably expressing APP_{WT} and BACE1 (Fig. 5). Analysis of transgenic γ-secretase subunits expression in HEK293 APP_{WT}/BACE1 stable cells (Fig. 5*A*) confirmed the maturation differences described for COS-7 cells (*i.e.* a lower degree of glycosylation of

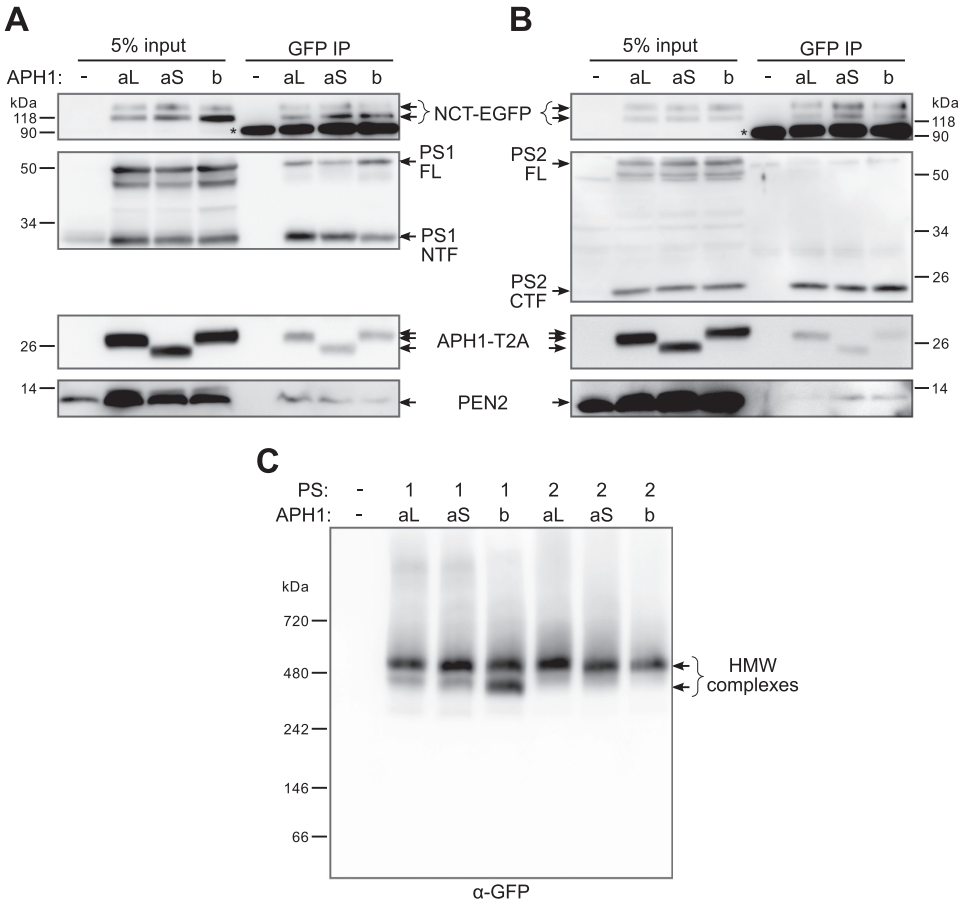

FIGURE 4. **γ-Secretase subunit interaction and assembly into high molecular weight complexes.** *A* and *B*, COS-7 cells were co-transfected with empty vector, or 4γ-PS1/APH1 constructs (*A*), or 4γ-PS2/APH1 constructs (*B*) and the transactivator-protein expression plasmid; transgene expression was induced with doxycycline for 5 h the next day, and cells were lysed in 1% CHAPSO buffer 1 day after induction and processed for immunoprecipitation using an anti-GFP antibody (*GFP IP*). The immunoprecipitation of NCT-EGFP and the co-immunoprecipitation of the γ-secretase components were analyzed by Western blot using specific antibodies for each γ-secretase subunit or an anti-GFP antibody to detect NCT-EGFP and an anti-2A peptide antibody to detect APH1-T2A. *, immunoglobulin heavy chain band. *C*, COS-7 cells were co-transfected and induced as in *A* and *B* and were processed to recover a membrane-enriched fraction 1 day after induction, followed by solubilization in a 1% digitonin buffer. Solubilized proteins were separated by blue native PAGE followed by Western blot using an anti-GFP antibody to detect native protein complexes where NCT-EGFP was incorporated. *HMW,* high molecular weight.

NCT-EGFP and reduced PS1 endoproteolysis in 4γ-PS1/APH1b-transfected cells and, more broadly, a lower level of PS endoproteolysis in cells transfected with PS1- *versus* PS2-containing constructs). Overall, our data indicate that the maturation/endoproteolysis differences observed in 4γ-PS/APH1-transfected cells were not associated with cell-specific effects but genuinely linked to the nature of the heteromeric complexes.

Aβ40 secretion was significantly increased in HEK293 APP_{WT}/BACE1 cells transfected with any 4γ-PS1/APH1 construct (Fig. 5*B*), whereas it appeared similar to control in all 4γ-PS2/APH1-transfected cells. These results support our *in vitro* observations in COS-7 cells of a lower activity of PS2-containing γ-secretase complexes as compared with PS1-containing complexes.

Aβ42 secretion was significantly increased in 4γ-PS1/APH1aS- and 4γ-PS1/APH1b-transfected cells, whereas 4γ-PS1/APH1aL-transfected cells and any 4γ-PS2/APH1-transfected cells secreted similar levels of Aβ42 as compared with empty vector-transfected cells, which were all significantly lower as compared with the levels of 4γ-PS1/APH1aS- or 4γ-PS1/APH1b-transfected cells (Fig. 5*C* and Table 1).

We next calculated and compared the Aβ42/Aβ40 ratios obtained with the different transfections (Fig. 5*D*), and we noticed that the nature of the co-expressed APH1 subunit was the main determinant of the observed variations. Thus, 4γ-PS1/APH1aL- and 4γ-PS2/APH1aL-transfected cells presented similar Aβ42/Aβ40 ratios that were lower than the empty vector-transfected cell ratio. 4γ-PS1/APH1aS- and 4γ-PS2/APH1aS-transfected cells presented Aβ42/Aβ40 ratios that were comparable with that of empty vector-transfected cells, whereas 4γ-PS1/APH1b- and 4γ-PS2/APH1b-transfected cells presented similar Aβ42/Aβ40 ratios that were higher than in empty vector-transfected cells. Even if these differences did not reach statistical significance, the Aβ42/Aβ40 ratios from 4γ-PS1/APH1aL- or 4γ-PS2/APH1aL-transfected cells were significantly different from those of 4γ-PS1/APH1b- or 4γ-PS2/APH1b-transfected cells (Table 1).

Thus, despite an endogenous set of γ-secretase activities in HEK293 APP_{WT}/BACE1 stable cells, we were able to delineate striking APH1 component-related differences in the Aβ42/Aβ40 ratios. In particular, cells transfected with APH1b-containing constructs presented significantly higher Aβ42/Aβ40 ratios than those transfected with APH1aL-containing con-

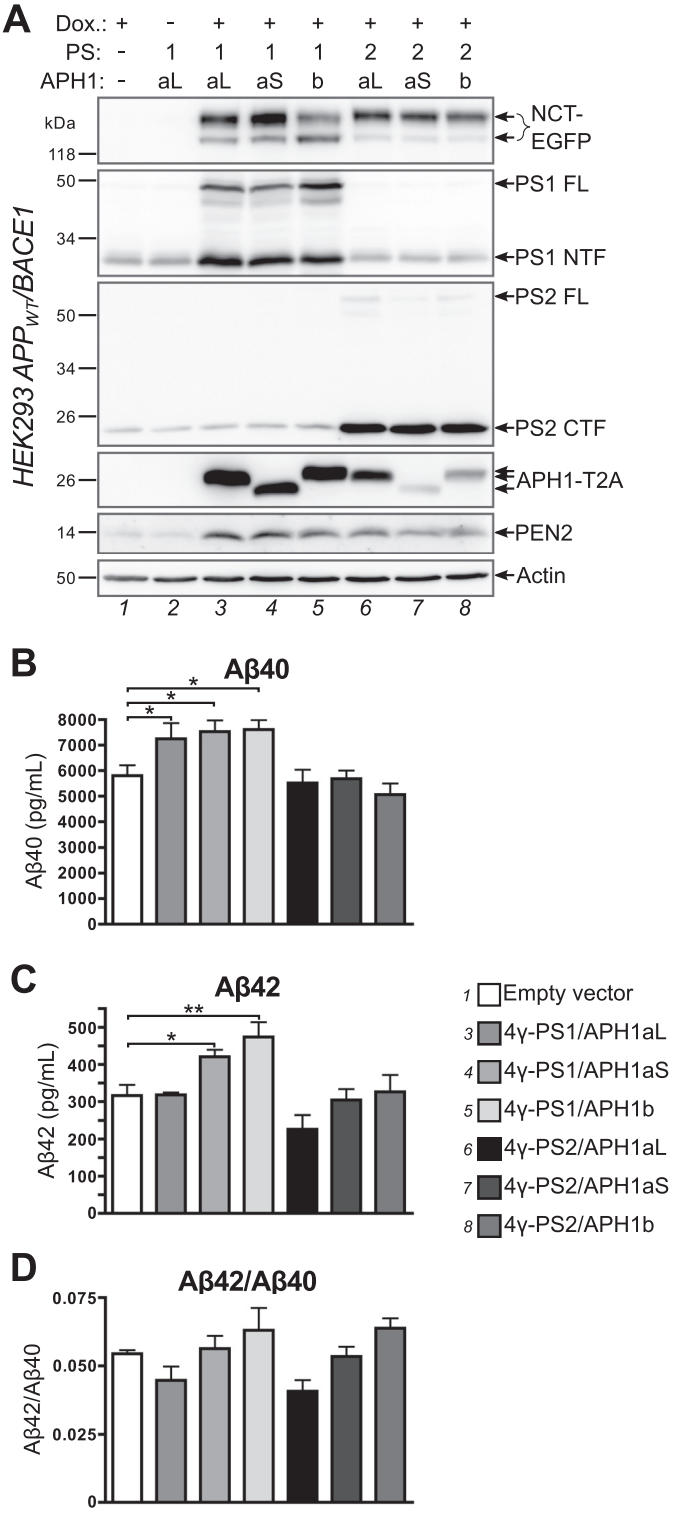

FIGURE 5. **Modifications of amyloid peptides secretion by specific γ-secretase complexes.** HEK293 cells stably expressing APP_{WT} and BACE1 were co-transfected with empty vector or with the indicated 4γ-PS/APH1 constructs and the transactivator protein expression plasmid; 7 h after transfection, transgene expression was induced or not with doxycycline (*Dox.*) for 16 h; 8 h after induction, cells were placed for 16 h in secretion medium, which was collected prior to cell lysis. *A*, cell lysates were analyzed by Western blot using specific antibodies for each γ-secretase subunit or an anti-GFP antibody to detect NCT-EGFP and an anti-2A peptide antibody to detect APH1-T2A. *B–D*, secretion media were analyzed by ELISA to measure secreted Aβ40 (*B*) and secreted Aβ42 (*C*), and the Aβ42/Aβ40 ratio was then calculated (*D*). Results are presented as mean ± S.E. (*error bars*) ($n = 3$). Statistical analysis using repeated measures analysis of variance revealed that means for secreted Aβ40, secreted Aβ42, and the Aβ42/Aβ40 ratio were significantly different ($p = 0.0015$, 0.0002, and 0.0069, respectively), Newman-Keuls multiple comparison tests reveal significant differences between control cells transfected with empty vector and those transfected with 4γ-PS1/APH1 constructs where indicated (*, $p < 0.05$; **, $p < 0.01$). The full results of Newman-Keuls pairwise comparisons are presented in Table 1.

TABLE 1

Newman-Keuls pairwise comparison results for Fig. 3 (*C* and *D*) and Fig. 5 (*B–D*)

For clarity, empty vector-transfected cells are designated as "v", and 4γ-PS/APH1-transfected cells are identified with presenilin number and APH1 variant letters (*e.g.* 1aL represents 4γ-PS1/APH1aL). NS, not significant ($p > 0.05$).

	Fig. 3		Fig. 5		
	AICD	Aβ	Aβ40	Aβ42	Aβ42/Aβ40
v *vs.* 1aL	$p < 0.05$	$p < 0.01$	$p < 0.05$	NS	NS
v *vs.* 1aS	$p < 0.05$	$p < 0.01$	$p < 0.05$	$p < 0.05$	NS
v *vs.* 1b	$p < 0.05$	$p < 0.01$	$p < 0.05$	$p < 0.01$	NS
v *vs.* 2aL	NS	NS	NS	NS	NS
v *vs.* 2aS	NS	NS	NS	NS	NS
v *vs.* 2b	NS	NS	NS	NS	NS
1aL *vs.* 1aS	NS	NS	NS	$p < 0.05$	NS
1aL *vs.* 1b	NS	NS	NS	$p < 0.01$	$p < 0.05$
1aL *vs.* 2aL	NS	$p < 0.05$	$p < 0.05$	NS	NS
1aL *vs.* 2aS	$p < 0.05$	$p < 0.05$	$p < 0.05$	NS	NS
1aL *vs.* 2b	NS	$p < 0.05$	$p < 0.05$	NS	$p < 0.05$
1aS *vs.* 1b	NS	NS	NS	NS	NS
1aS *vs.* 2aL	NS	NS	$p < 0.05$	$p < 0.01$	NS
1aS *vs.* 2aS	$p < 0.05$	NS	$p < 0.05$	$p < 0.05$	NS
1aS *vs.* 2b	NS	NS	$p < 0.01$	$p < 0.05$	NS
1b *vs.* 2aL	NS	NS	$p < 0.05$	$p < 0.001$	$p < 0.05$
1b *vs.* 2aS	$p < 0.05$	NS	$p < 0.05$	$p < 0.01$	NS
1b *vs.* 2b	NS	NS	$p < 0.01$	$p < 0.01$	NS
2aL *vs.* 2aS	NS	NS	NS	NS	NS
2aL *vs.* 2b	NS	NS	NS	NS	$p < 0.05$
2aS *vs.* 2b	NS	NS	NS	NS	NS

structs (Fig. 5*D* and Table 1). These observations are in full accordance with those of Acx *et al.* (59), who showed, in a γ-secretase null background, that APH1b-containing γ-secretase complexes favored the production of longer Aβ peptides as compared with their APH1aL-containing counterparts. These results therefore further identify our 4γ-PS/APH1 constructs as appropriate tools to yield functional γ-secretase complexes harboring their proper enzymatic activities and, thus, to examine their cellular trafficking.

We also tested our 4γ-PS/APH1 constructs in HEK293 cells stably expressing mΔENotch (66). Western blot analysis did not reveal alteration in the processing of this substrate NICD (Notch intracellular domain)/mΔENotch ratio (supplemental Fig. S1). However, we cannot exclude the possibility that subtle changes may not be detected due to the lower sensitivity of this approach (as compared with the ELISA measurements of Aβ peptide secretion) and to the fact that these cells display endogenous γ-secretase.

PS1- and PS2-containing γ-Secretase Complexes Are Targeted to Distinct Subcellular Compartments—Are γ-secretase complexes of different compositions targeted to distinct cellular compartments? To address this question, we first transfected COS-7 cells with the various 4γ-PS/APH1 constructs and transiently induced γ-secretase expression 1 day before microscope observation. In all 4γ-PS1/APH1-transfected cells, NCT-EGFP fluorescence was mainly detected at the plasma membrane, thereby delineating the contours of the cells (Fig. 6*A*). Whereas some cells presented only this cell surface fluorescence (such as the one presented in Fig. 2*B*), other cells still displayed some fluorescence probably associated with the ER,

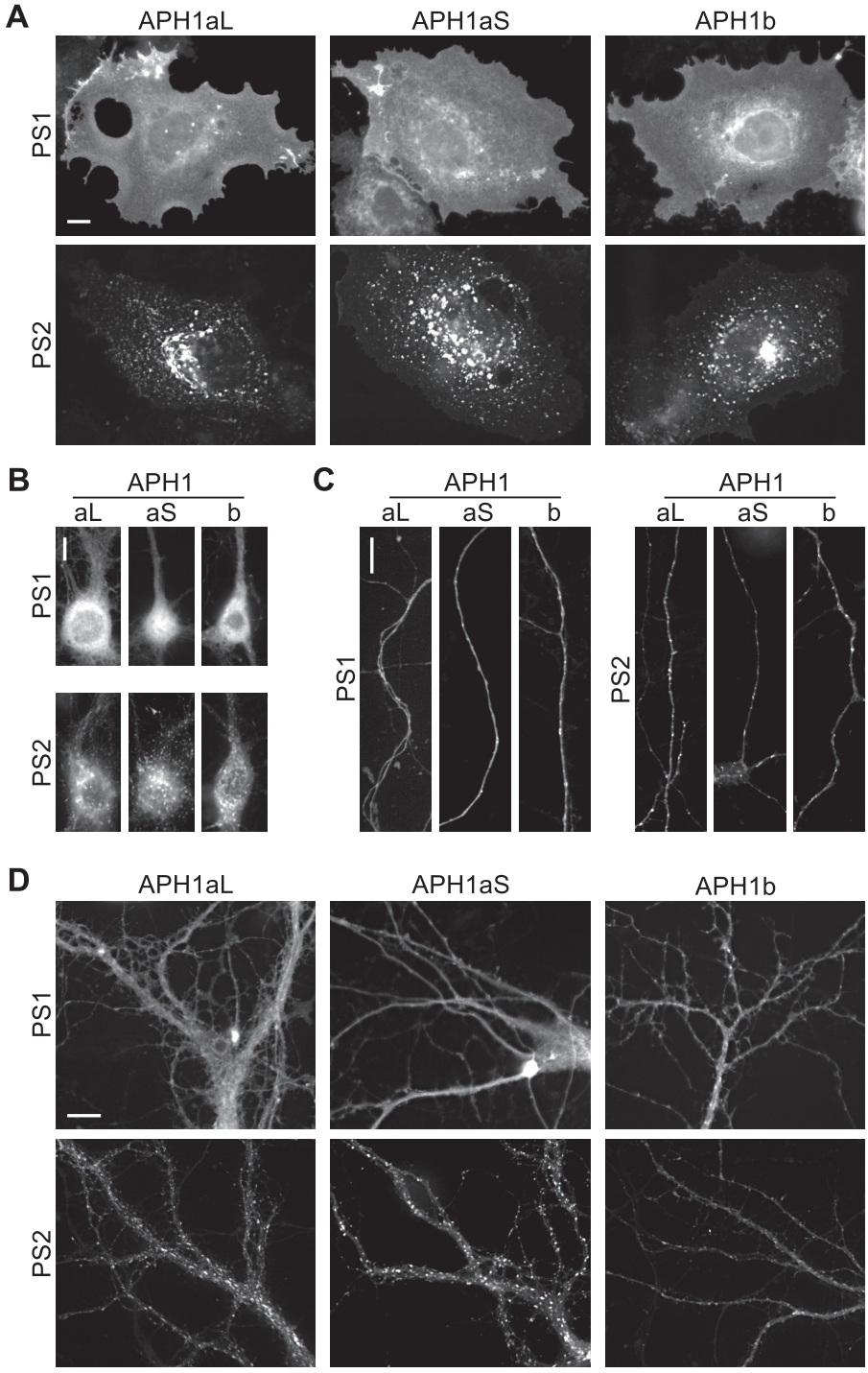

FIGURE 6. **PS1- and PS2- containing γ-secretase complexes are targeted to distinct cellular compartments.** *A*, COS-7 cells were co-transfected with 4γ-PS/APH1 constructs (the specific PS and APH1 subunits are indicated on the *left* and *top* of images, respectively), and the transactivator protein expression plasmid; transgene expression was induced with doxycycline for 2 h the next day, cells were fixed 1 day after induction, and EGFP fluorescence was acquired using wide field epifluorescence microscopy. *B–D*, primary hippocampal neurons from embryonic (embryonic day 18) rats were transfected with 4γ-PS/APH1 constructs (the variable subunits are indicated on the *left* (PS) and the *top* (APH1) of each *panel*), and the transactivator protein expression plasmid at 6 DIV, induced with doxycycline at 16 DIV for 5 h, and fixed the following day before observation of EGFP signal in the soma (*B*), the axon (*C*), and dendrites (*D*) of transfected neurons using wide field epifluorescence microscopy. *Scale bars*, 10 μm.

in continuity with the nuclear envelope, especially in 4γ-PS1/APH1b- transfected cells. Strikingly, in 4γ-PS2/APH1-expressing cells, NCT-EGFP fluorescence was concentrated in intracellular organelles, presenting mostly a vesicular aspect but also sometimes a tubular appearance (Fig. 6*A*). Two main patterns of distribution were observed for all 4γ-PS2/APH1-transfected cells: 1) several large vesicular structures near one side of the nucleus and many other smaller vesicles scattered throughout the cell (Fig. 6*A*, *bottom left* and *middle panels*) or 2) one large and bright structure near the nucleus and numerous small vesicles scattered throughout the cell (Fig. 6*A*, *bottom right*). Occasionally, faint fluorescence was also detected at the cell surface,

suggesting that PS2-containing γ-secretase complexes may transit through the plasma membrane before reaching the intracellular structures where they accumulate. In addition, no ER-associated NCT-EGFP fluorescence was visible around the cell nucleus in the cells transfected with PS2-containing constructs. When observed by time lapse video microscopy, these intracellular structures appeared to display different dynamics, depending on their pattern of distribution (described above; supplemental Movie 1), with some cells presenting more tubules able to bend, split, and turn within the cell (supplemental Movie 2). These strikingly distinct repartitions of NCT-EGFP fluorescence in 4γ-PS1/APH1- and 4γ-PS2/APH1-transfected cells confirmed that the observed fluorescence indeed came from NCT-EGFP incorporated into newly assembled γ-secretase complexes and did not correspond to free, unassembled NCT-EGFP.

According to the likely contribution of γ-secretase in Alzheimer disease, we assessed the relevance of our observation by examining the distribution of PS1- and PS2-containing γ-secretase complexes in primary cultured hippocampal neurons. A homogeneous cell surface-associated fluorescence was observed in the soma, axons, and dendrites of neurons transfected with all 4γ-PS1/APH1 constructs (Fig. 6, *B–D*, respectively). In addition, these neurons presented NCT-EGFP fluorescence around the nucleus (Fig. 6*B*), reminiscent of the ER-associated fluorescence observed in COS-7 cells. In neurons transfected with PS2-containing constructs, NCT-EGFP fluorescence was concentrated in intracellular vesicular structures throughout the soma, axons, and dendrites (Fig. 6, *B–D*). Therefore, the PS-related distinct distributions observed in COS-7 cells fully stand in cultured neurons, indicating that they could not be accounted for by cell-specific effects and appear relevant with regard to AD brain pathology.

PS2-containing γ-Secretase Complexes Are Located in the trans-Golgi Network and in Distinct Subsets of Endosomal Compartments, Depending on Their Associated APH1 Subunit—To identify the intracellular compartments where PS2-containing γ-secretase complexes are targeted, we performed immunocytochemistry experiments using several organelle markers in COS-7 cells transfected with 4γ-PS2/APH1 constructs. NCT-EGFP fluorescence in large vesicular or tubulo-vesicular structures near the nucleus overlapped substantially with the *trans*-Golgi network (TGN) marker TGN46 in 4γ-PS2/APH1aL- or 4γ-PS2/APH1b-transfected cells (Fig. 7*A*). This overlap was only partial in 4γ-PS2/APH1aS-transfected cells. NCT-EGFP fluorescence in the other vesicular structures overlapped partially with the early endosome marker EEA1 (supplemental Fig. S2) and co-localized more substantially with the recycling endosome marker transferrin receptor (Fig. 7*B*, *TfR*) in all 4γ-PS2/APH1-transfected cells. Several NCT-EGFP-labeled vesicles co-localized with the late endosomes-associated tetraspanin CD63 (67) in 4γ-PS2/APH1aS- and 4γ-PS2/APH1b-transfected cells but not in 4γ-PS2/APH1aL-transfected cells (Fig. 7*C*). Similarly, some larger "donut-shaped" vesicular structures labeled by NCT-EGFP fluorescence appeared to be filled by the lysosome marker Lysotracker Red in 4γ-PS2/APH1aS- and 4γ-PS2/APH1b-transfected cells but not in 4γ-PS2/APH1aL-transfected cells (Fig. 7*D*). Altogether, these results demonstrate that PS2-containing γ-secretase complexes are present in the TGN and in multiple endosomal compartments and are particularly enriched in recycling endosomes.

Discussion

In the present study, we generate new constructs to transiently induce the stoichiometric co-expression of the four core components of γ-secretase complexes with specific combinations of their variable subunits presenilin and APH1 and to visualize their cellular trafficking through the EGFP-tagged nicastrin incorporated in newly formed complexes. Interestingly, the biochemical characterization of these tools reveals different composition-dependent rates of maturation of the complexes into functional γ-secretase. Strikingly, PS1-containing complexes are mainly targeted to the plasma membrane, whereas PS2-containing complexes are addressed to the TGN and a subset of endosomal compartments and are particularly enriched in recycling endosomes. Additionally, cellular distribution of PS2-containing complexes differs according to the APH1 component. Thus, PS2/APH1aS- or PS2/APH1b-containing complexes are also observed in late endosomes and lysosomes in which PS2/APH1aL-containing complexes were never detected.

Differential Maturation Rates of γ-Secretase Complexes Depending on Their Composition—One main advantage of our constructs is that they allow us to transiently synthesize γ-secretase subunits through doxycycline induction in a few hours, thereby allowing observation of their expression at a given time after the end of induction. We mostly analyzed γ-secretase subunit expression between 20 and 22 h after the end of induction to permit their assembly, maturation, and trafficking outside the ER where they are synthesized. Using these settings, and despite the optimized design of our constructs for the stoichiometric expression of the four γ-secretase subunits, we still detect full-length PS1 and PS2, showing that a fraction of transfected presenilins was not endoproteolyzed. Surprisingly, this fraction is more important for PS1-containing γ-secretase complexes than for those containing PS2. This observation suggests a less efficient endoproteolysis of PS1 *versus* PS2 or a slower assembly of PS1-containing γ-secretase complexes. This latter explanation is corroborated by the detection of smaller intermediate complexes in 4γ-PS1/APH1-transfected cells in addition to the main high molecular mass complexes (>480 kDa) that are the only ones observed in 4γ-PS2/APH1-transfected cells. This interpretation is further strengthened by the observation of a residual ER-associated NCT-EGFP fluorescence in the cells transfected with PS1-containing constructs that may correspond to partially assembled complexes and that is absent in the cells transfected with PS2-containing constructs.

The levels of full-length PS1 are even higher in cells transfected with 4γ-PS1/APH1b that also presented a lower degree of NCT-EGFP glycosylation. This result suggests a higher degree of ER retention/retrieval of PS1- and APH1b-containing γ-secretase complexes, and accordingly, 4γ-PS1/APH1b-transfected cells present a more intense ER-associated NCT-EGFP fluorescence. These results corroborate our previous findings,

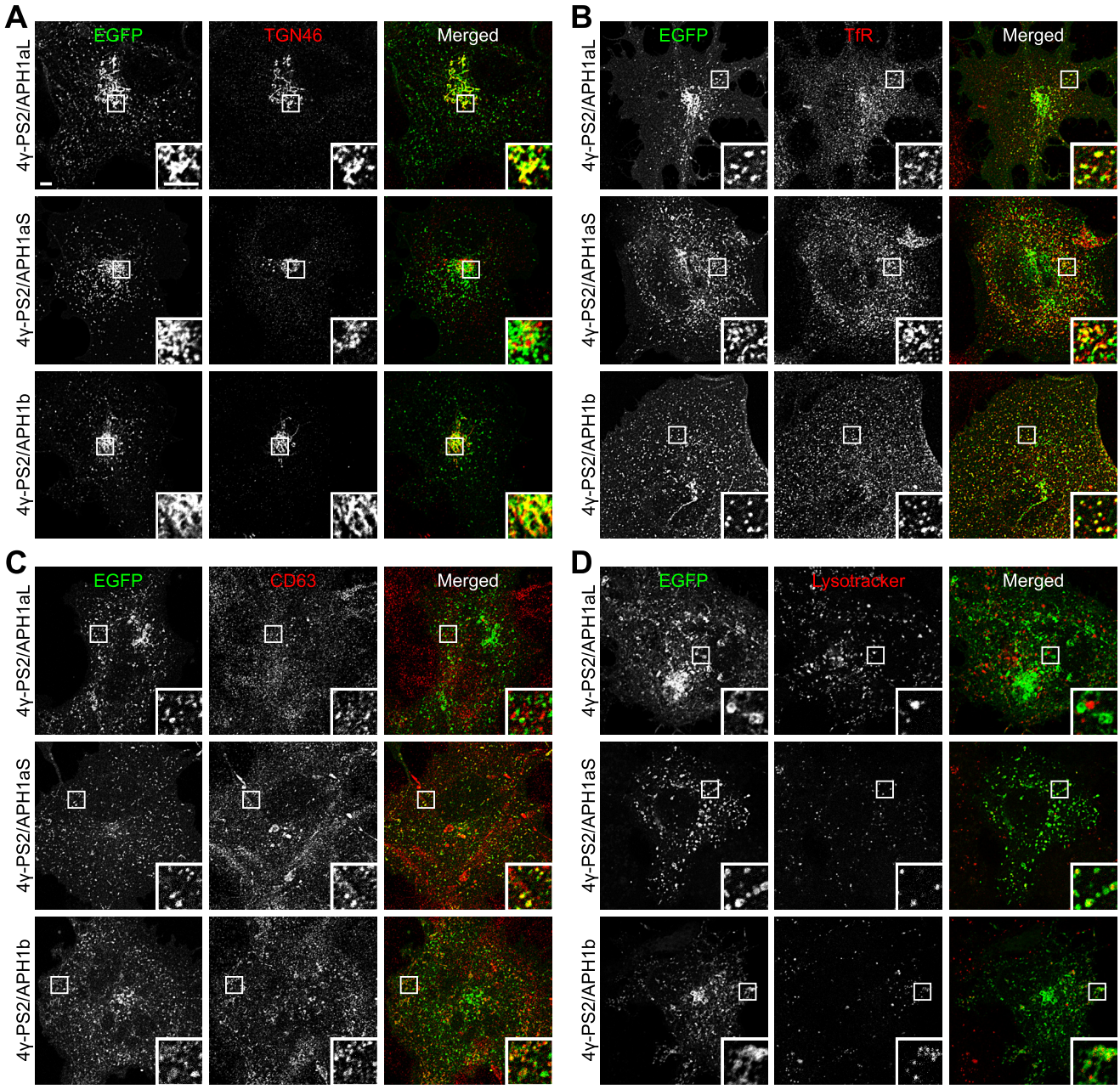

FIGURE 7. **PS2-containing γ-secretase complexes are present in the *trans*-Golgi network and in multiple endosomal compartments.** *A–D*, COS-7 cells were co-transfected with the indicated 4γ-PS2/APH1 constructs and the transactivator protein expression plasmid; transgene expression was induced with doxycycline for 2 h the next day, and cells were fixed 1 day after induction and processed for immunocytochemistry using antibodies against the *trans*-Golgi network marker TGN46 (*A*), the recycling endosome marker transferrin receptor (*TfR* (*B*)), or the late endosome marker CD63 (*C*). Alternatively, cells were labeled with Lysotracker Red prior to fixation (*D*). Fluorescent signals were acquired using laser confocal microscopy. *Insets*, magnifications of the *boxed areas*. *Scale bars*, 5 μm.

obtained with different constructs driving a continuous expression of BiFC-tagged γ-secretase subunits, showing a higher ER retention/retrieval of γ-secretase complexes containing PS1 and APH1b than those containing PS1 and APH1aL or APH1aS (36). Interestingly, this lower level of nicastrin glycosylation of PS1/APH1b-containing γ-secretase complexes is also observed, but is not specifically discussed, by Acx *et al.* (59), who rescued PS/APH1s knock-out mouse embryonic fibroblasts with stable expression of specific combinations of human PS1 or PS2 and human APH1aL or APH1b. It remains to be determined whether PS1- and APH1b-containing γ-secretase complexes serve a particular function within the ER or whether additional signaling/stimuli can trigger/facilitate the ER exit of these complexes.

Differential Subcellular Targeting of γ-Secretase Complexes Depending on Their Presenilin Subunit—We demonstrate for the first time a striking difference in the subcellular targeting of PS1-containing γ-secretase complexes that are enriched in the plasma membrane and PS2-containing complexes that are addressed to the TGN and a subset of endosomes. This difference has obvious implications for the substrate specificity of PS1- or PS2-containing γ-secretase complexes. Indeed, the

regulated intramembrane proteolysis of γ-secretase substrates requires a rate-limiting cleavage resulting in the shedding of their ectodomain (4). The cellular site for this precleavage and the events immediately following it (such as the endocytosis of the cleaved substrate) probably influence the susceptibility of the substrate to further processing by PS1- or PS2-containing γ-secretase complexes. Similarly, the location of the γ-secretase cleavage, at the plasma membrane or in endosomal compartments, may influence the signaling efficiency of the generated intracellular domain. For example, the nuclear translocation and signaling of AICD require endocytosis (68, 69).

The detection of PS1-containing γ-secretase complexes at the plasma membrane is in agreement with our previous results obtained with BiFC-tagged γ-secretase subunits (36) as well as the results obtained by Kaether *et al.* (29) with HEK293 cells stably expressing EGFP-tagged PS1. It also agrees well with cell surface biotinylation data showing the presence of PS1 at the plasma membrane in different cell systems (28, 29, 70–74).

The subcellular localization of PS2 is much more poorly documented. We describe here the targeting of PS2-containing γ-secretase complexes to the TGN and a subset of endosomes with a particular enrichment in transferrin receptor-positive recycling endosomes, whatever the nature of their APH1 subunit. The presence of active PS2-containing γ-secretase complexes in the TGN is corroborated by the comparable increased production of Aβ42 in cells co-expressing mutant PS2 and an APP-C100 substrate tagged or not with a TGN-targeting sequence (75). Our live cell imaging experiments also reveal the presence of PS2-containing γ-secretase complexes in tubular structures that are characteristics of the recycling endosomes and are often lost during paraformaldehyde fixation. Supporting this localization, the hydrophilic loop of presenilins was shown to interact with Rab11, a GTPase associated with recycling endosomes, that is efficiently co-immunoprecipitated with PS2 in COS cells (76, 77). Interestingly, transferrin recycling is delayed by the pharmacological inhibition of γ-secretase or in PS1- and PS2-deficient embryonic stem cells, suggesting that presenilins may regulate recycling endosome function (70). In addition, we detected some PS2-containing γ-secretase complexes in organelles labeled with late endosome/lysosome markers when they also contain APH1aS or APH1b but not APH1aL, showing that the nature of the APH1 subunit can modulate the endocytic itineraries of PS2-containing γ-secretase complexes. In agreement with an increased abundance of PS2-containing γ-secretase complexes in intracellular compartments as compared with PS1-containing ones, higher intracellular accumulation of Aβ42 was observed in cells expressing familial AD mutant PS2 rather than mutant PS1 (78).

The localizations of PS1- and PS2-containing γ-secretase complexes revealed by our 4γ-PS/APH1 constructs seem in apparent contradiction with the results we obtained on APP processing, considering current knowledge on the subcellular sites for Aβ production. Indeed, many studies show that Aβ is generated mainly in the TGN and endosomes, where the β-secretase BACE1 is also found (79, 80). We observed an increased secretion of Aβ peptides only with the expression of PS1-containing γ-secretases (Fig. 5) that we found to be present at the plasma membrane (Fig. 6) and no significant variation of this secretion with the expression of PS2-containing γ-secretases that are actually targeted to the TGN and endosomes (Fig. 7). We cannot exclude the possibility that a portion of the total Aβ peptides generated were missed in our experiments, because we measured secreted Aβ but did not assess intracellular Aβ. However, during these experiments, a substantial part of the content of the TGN and endosomes should have been released in the extracellular medium through vesicular recycling. Furthermore, *in vitro* γ-secretase assays (Fig. 3), in which access to the substrate is not restricted by subcellular localization, confirm previous findings by other groups of the lower efficiency of PS2-containing γ-secretase complexes to process APP β-CTFs (59, 63, 64). This characteristic also probably contributes to the lower Aβ peptide secretion obtained with these complexes. Therefore, our results argue for the production of Aβ peptides at the plasma membrane by PS1-containing γ-secretase complexes, in agreement with reports from other groups (28, 32, 81)who notably showed that the inhibition of endocytosis did not prevent γ-secretase processing of β-CTFs and even increased Aβ secretion. Our results highlight an unexpected degree of complexity in the understanding of the γ-secretase processing of a particular substrate; not only the subcellular site(s) where this substrate is produced (*i.e.* where ectodomain shedding occurs) and the cellular localization of a specific γ-secretase complex should be considered, but also the relative affinity/efficiency of a specific γ-secretase complex to process this particular substrate. It will be interesting to further explore the physiological relevance of the sequential processing of APP by β- and γ-secretases along the endocytic/recycling routes and whether APP metabolites can inform the cell of the intensity of these vesicular turnovers.

New Relevant Tools to Decipher the Details of γ-Secretase Complex Trafficking—Our new constructs are designed for an inducible, temporary, and stoichiometric expression of specific combinations of the four γ-secretase subunits. We demonstrate here that these constructs allow for the formation of functional γ-secretase complexes displaying the major characteristics associated with their specific presenilin and APH1 content that were described recently (59) and their visualization in distinct cellular compartments. These tools will therefore be very useful to address the many remaining questions related to the trafficking of the different γ-secretase complexes and their substrates in cell lines and in primary neuronal cultures. Our constructs can be easily modified or implemented to study specific aspects of γ-secretase trafficking and to determine the molecular determinants of their differential targeting evidenced here. For example, it will be particularly interesting to study whether some mutations associated with familial forms of AD on PS1 or PS2 can affect the trafficking of the γ-secretase complexes in which these mutated subunits are incorporated. Our constructs are also well suited for live imaging of γ-secretase trafficking and will be useful to determine whether this trafficking can be altered by specific stimuli, notably in primary neuronal cultures. For instance, the activation of β_2-adrenergic receptors or δ-opioid receptors triggers the targeting of γ-secretase to late endosomes and lysosomes (82).

Finally, because multiple reports have demonstrated that neuronal activity modulates Aβ production and synaptic release (83–85), our tools will be helpful to determine the importance of γ-secretase trafficking in these processes in future studies.

Author Contributions—X. M. designed, performed, and analyzed experiments. X. M. and F. C. discussed data and wrote the manuscript.

Acknowledgments—We thank Dr. Frédéric Brau at the imaging facility of the Institute for Molecular and Cellular Pharmacology (IPMC, CNRS UMR7275) for help with fluorescence microscopy. We thank Dr. Michel Franco and Dr. Bruno Mesmin (IPMC) for providing antibodies against protein markers for different cellular organelles.

References

1. Bohm, C., Chen, F., Sevalle, J., Qamar, S., Dodd, R., Li, Y., Schmitt-Ulms, G., Fraser, P. E., and St George-Hyslop, P. H. (2015) Current and future implications of basic and translational research on amyloid-β peptide production and removal pathways. *Mol. Cell Neurosci.* **66,** 3–11
2. Doody, R. S., Raman, R., Farlow, M., Iwatsubo, T., Vellas, B., Joffe, S., Kieburtz, K., He, F., Sun, X., Thomas, R. G., Aisen, P. S., Alzheimer's Disease Cooperative Study Steering Committee, Siemers, E., Sethuraman, G., Mohs, R., and Semagacestat Study Group (2013) A phase 3 trial of semagacestat for treatment of Alzheimer's disease. *N. Engl. J. Med.* **369,** 341–350
3. Mikulca, J. A., Nguyen, V., Gajdosik, D. A., Teklu, S. G., Giunta, E. A., Lessa, E. A., Tran, C. H., Terak, E. C., and Raffa, R. B. (2014) Potential novel targets for Alzheimer pharmacotherapy: II. update on secretase inhibitors and related approaches. *J. Clin. Pharm. Ther.* **39,** 25–37
4. McCarthy, J. V., Twomey, C., and Wujek, P. (2009) Presenilin-dependent regulated intramembrane proteolysis and γ-secretase activity. *Cell Mol. Life Sci.* **66,** 1534–1555
5. Haapasalo, A., and Kovacs, D. M. (2011) The many substrates of presenilin/γ-secretase. *J. Alzheimers Dis.* **25,** 3–28
6. Edbauer, D., Winkler, E., Regula, J. T., Pesold, B., Steiner, H., and Haass, C. (2003) Reconstitution of γ-secretase activity. *Nat. Cell Biol.* **5,** 486–488
7. Kimberly, W. T., LaVoie, M. J., Ostaszewski, B. L., Ye, W., Wolfe, M. S., and Selkoe, D. J. (2003) γ-Secretase is a membrane protein complex comprised of presenilin, nicastrin, Aph-1, and Pen-2. *Proc. Natl. Acad. Sci. U.S.A.* **100,** 6382–6387
8. Takasugi, N., Tomita, T., Hayashi, I., Tsuruoka, M., Niimura, M., Takahashi, Y., Thinakaran, G., and Iwatsubo, T. (2003) The role of presenilin cofactors in the γ-secretase complex. *Nature* **422,** 438–441
9. Sato, T., Diehl, T. S., Narayanan, S., Funamoto, S., Ihara, Y., De Strooper, B., Steiner, H., Haass, C., and Wolfe, M. S. (2007) Active γ-secretase complexes contain only one of each component. *J. Biol. Chem.* **282,** 33985–33993
10. Osenkowski, P., Li, H., Ye, W., Li, D., Aeschbach, L., Fraering, P. C., Wolfe, M. S., Selkoe, D. J., and Li, H. (2009) Cryoelectron microscopy structure of purified γ-secretase at 12 Å resolution. *J. Mol. Biol.* **385,** 642–652
11. Yu, G., Nishimura, M., Arawaka, S., Levitan, D., Zhang, L., Tandon, A., Song, Y. Q., Rogaeva, E., Chen, F., Kawarai, T., Supala, A., Levesque, L., Yu, H., Yang, D. S., Holmes, E., *et al.* (2000) Nicastrin modulates presenilin-mediated notch/glp-1 signal transduction and betaAPP processing. *Nature* **407,** 48–54
12. Goutte, C., Tsunozaki, M., Hale, V. A., and Priess, J. R. (2002) APH-1 is a multipass membrane protein essential for the Notch signaling pathway in *Caenorhabditis elegans* embryos. *Proc. Natl. Acad. Sci. U.S.A.* **99,** 775–779
13. Francis, R., McGrath, G., Zhang, J., Ruddy, D. A., Sym, M., Apfeld, J., Nicoll, M., Maxwell, M., Hai, B., Ellis, M. C., Parks, A. L., Xu, W., Li, J., Gurney, M., Myers, R. L., Himes, C. S., Hiebsch, R., Ruble, C., Nye, J. S., and Curtis, D. (2002) aph-1 and pen-2 are required for Notch pathway signaling, γ-secretase cleavage of βAPP, and presenilin protein accumulation. *Dev. Cell* **3,** 85–97
14. Rogaev, E. I., Sherrington, R., Rogaeva, E. A., Levesque, G., Ikeda, M., Liang, Y., Chi, H., Lin, C., Holman, K., and Tsuda, T. (1995) Familial Alzheimer's disease in kindreds with missense mutations in a gene on chromosome 1 related to the Alzheimer's disease type 3 gene. *Nature* **376,** 775–778
15. Sherrington, R., Rogaev, E. I., Liang, Y., Rogaeva, E. A., Levesque, G., Ikeda, M., Chi, H., Lin, C., Li, G., Holman, K., Tsuda, T., Mar, L., Foncin, J. F., Bruni, A. C., Montesi, M. P., Sorbi, S., Rainero, I., Pinessi, L., Nee, L., Chumakov, I., Pollen, D., Brookes, A., Sanseau, P., Polinsky, R. J., Wasco, W., Da Silva, H. A., Haines, J. L., Perkicak-Vance, M. A., Tanzi, R. E., Roses, A. D., Fraser, P. E., Rommens, J. M., and St George-Hyslop, P. H. (1995) Cloning of a gene bearing missense mutations in early-onset familial Alzheimer's disease. *Nature* **375,** 754–760
16. Wolfe, M. S., Xia, W., Ostaszewski, B. L., Diehl, T. S., Kimberly, W. T., and Selkoe, D. J. (1999) Two transmembrane aspartates in presenilin-1 required for presenilin endoproteolysis and γ-secretase activity. *Nature* **398,** 513–517
17. Thinakaran, G., Borchelt, D. R., Lee, M. K., Slunt, H. H., Spitzer, L., Kim, G., Ratovitsky, T., Davenport, F., Nordstedt, C., Seeger, M., Hardy, J., Levey, A. I., Gandy, S. E., Jenkins, N. A., Copeland, N. G., Price, D. L., and Sisodia, S. S. (1996) Endoproteolysis of presenilin 1 and accumulation of processed derivatives *in vivo*. *Neuron* **17,** 181–190
18. Capell, A., Beher, D., Prokop, S., Steiner, H., Kaether, C., Shearman, M. S., and Haass, C. (2005) γ-Secretase complex assembly within the early secretory pathway. *J. Biol. Chem.* **280,** 6471–6478
19. Kim, S.-H., Yin, Y. I., Li, Y.-M., and Sisodia, S. S. (2004) Evidence that assembly of an active γ-secretase complex occurs in the early compartments of the secretory pathway. *J. Biol. Chem.* **279,** 48615–48619
20. Kaether, C., Capell, A., Edbauer, D., Winkler, E., Novak, B., Steiner, H., and Haass, C. (2004) The presenilin C-terminus is required for ER-retention, nicastrin-binding and γ-secretase activity. *EMBO J.* **23,** 4738–4748
21. Kaether, C., Scheuermann, J., Fassler, M., Zilow, S., Shirotani, K., Valkova, C., Novak, B., Kacmar, S., Steiner, H., and Haass, C. (2007) Endoplasmic reticulum retention of the γ-secretase complex component Pen2 by Rer1. *EMBO Rep.* **8,** 743–748
22. Spasic, D., Raemaekers, T., Dillen, K., Declerck, I., Baert, V., Serneels, L., Füllekrug, J., and Annaert, W. (2007) Rer1p competes with APH-1 for binding to nicastrin and regulates γ-secretase complex assembly in the early secretory pathway. *J. Cell Biol.* **176,** 629–640
23. Fassler, M., Zocher, M., Klare, S., La Fuente, de la Fuente, A. G., Scheuermann, J., Capell, A., Haass, C., Valkova, C., Veerappan, A., Schneider, D., and Kaether, C. (2010) Masking of transmembrane-based retention signals controls ER export of γ-secretase. *Traffic* **11,** 250–258
24. Yang, D.-S., Tandon, A., Chen, F., Yu, G., Yu, H., Arawaka, S., Hasegawa, H., Duthie, M., Schmidt, S. D., Ramabhadran, T. V., Nixon, R. A., Mathews, P. M., Gandy, S. E., Mount, H. T. J., St George-Hyslop, P., and Fraser, P. E. (2002) Mature glycosylation and trafficking of nicastrin modulate its binding to presenilins. *J. Biol. Chem.* **277,** 28135–28142
25. Herreman, A., Van Gassen, G., Bentahir, M., Nyabi, O., Craessaerts, K., Mueller, U., Annaert, W., and De Strooper, B. (2003) gamma-Secretase activity requires the presenilin-dependent trafficking of nicastrin through the Golgi apparatus but not its complex glycosylation. *J. Cell Sci.* **116,** 1127–1136
26. Kaech, S., and Banker, G. (2006) Culturing hippocampal neurons. *Nat. Protoc.* **1,** 2406–2415
27. Schneider, C. A., Rasband, W. S., and Eliceiri, K. W. (2012) NIH Image to ImageJ: 25 years of image analysis. *Nat. Methods* **9,** 671–675
28. Chyung, J. H., Raper, D. M., and Selkoe, D. J. (2005) γ-secretase exists on the plasma membrane as an intact complex that accepts substrates and effects intramembrane cleavage. *J. Biol. Chem.* **280,** 4383–4392
29. Kaether, C., Lammich, S., Edbauer, D., Ertl, M., Rietdorf, J., Capell, A., Steiner, H., and Haass, C. (2002) Presenilin-1 affects trafficking and processing of βAPP and is targeted in a complex with nicastrin to the plasma membrane. *J. Cell Biol.* **158,** 551–561
30. Hansson, E. M., Strömberg, K., Bergstedt, S., Yu, G., Näslund, J., Lundkvist, J., and Lendahl, U. (2005) Aph-1 interacts at the cell surface with proteins in the active γ-secretase complex and membrane-tethered Notch. *J. Neurochem.* **92,** 1010–1020

31. Zeitelhofer, M., Vessey, J. P., Thomas, S., Kiebler, M., and Dahm, R. (2009) Transfection of cultured primary neurons via nucleofection. *Curr. Protoc. Neurosci.* 10.1002/0471142301.ns0432s47
32. Kaether, C., Schmitt, S., Willem, M., and Haass, C. (2006) Amyloid precursor protein and Notch intracellular domains are generated after transport of their precursors to the cell surface. *Traffic* **7,** 408–415
33. Vaccari, T., Lu, H., Kanwar, R., Fortini, M. E., and Bilder, D. (2008) Endosomal entry regulates Notch receptor activation in *Drosophila melanogaster*. *J. Cell Biol.* **180,** 755–762
34. Gupta-Rossi, N., Six, E., LeBail, O., Logeat, F., Chastagner, P., Olry, A., Israël, A., and Brou, C. (2004) Monoubiquitination and endocytosis direct γ-secretase cleavage of activated Notch receptor. *J. Cell Biol.* **166,** 73–83
35. Urra, S., Escudero, C. A., Ramos, P., Lisbona, F., Allende, E., Covarrubias, P., Parraguez, J. I., Zampieri, N., Chao, M. V., Annaert, W., and Bronfman, F. C. (2007) TrkA receptor activation by nerve growth factor induces shedding of the p75 neurotrophin receptor followed by endosomal γ-secretase-mediated release of the p75 intracellular domain. *J. Biol. Chem.* **282,** 7606–7615
36. Meckler, X., and Checler, F. (2014) Visualization of specific γ-secretase complexes using bimolecular fluorescence complementation. *J. Alzheimers Dis.* **40,** 161–176
37. Pasternak, S. H., Bagshaw, R. D., Guiral, M., Zhang, S., Ackerley, C. A., Pak, B. J., Callahan, J. W., and Mahuran, D. J. (2003) Presenilin-1, nicastrin, amyloid precursor protein, and γ-secretase activity are co-localized in the lysosomal membrane. *J. Biol. Chem.* **278,** 26687–26694
38. Tam, J. H. K., Seah, C., and Pasternak, S. H. (2014) The amyloid precursor protein is rapidly transported from the Golgi apparatus to the lysosome and where it is processed into β-amyloid. *Mol. Brain* **7,** 54
39. Alzheimer's Disease Collaborative Group (1995) The structure of the presenilin 1 (S182) gene and identification of six novel mutations in early onset AD families. *Nat. Genet.* **11,** 219–222
40. Gu, Y., Chen, F., Sanjo, N., Kawarai, T., Hasegawa, H., Duthie, M., Li, W., Ruan, X., Luthra, A., Mount, H. T. J., Tandon, A., Fraser, P. E., and St George-Hyslop, P. (2003) APH-1 interacts with mature and immature forms of presenilins and nicastrin and may play a role in maturation of presenilin·nicastrin complexes. *J. Biol. Chem.* **278,** 7374–7380
41. Shirotani, K., Edbauer, D., Prokop, S., Haass, C., and Steiner, H. (2004) Identification of distinct γ-secretase complexes with different APH-1 variants. *J. Biol. Chem.* **279,** 41340–41345
42. Hébert, S. S., Serneels, L., Dejaegere, T., Horré, K., Dabrowski, M., Baert, V., Annaert, W., Hartmann, D., and De Strooper, B. (2004) Coordinated and widespread expression of γ-secretase *in vivo*: evidence for size and molecular heterogeneity. *Neurobiol. Dis.* **17,** 260–272
43. Szymczak-Workman, A. L., Vignali, K. M., and Vignali, D. A. A. (2012) Design and construction of 2A peptide-linked multicistronic vectors. *Cold Spring Harbor Protocols.* **2012,** 199–204
44. Hasegawa, H., Sanjo, N., Chen, F., Gu, Y.-J., Shier, C., Petit, A., Kawarai, T., Katayama, T., Schmidt, S. D., Mathews, P. M., Schmitt-Ulms, G., Fraser, P. E., and St George-Hyslop, P. (2004) Both the sequence and length of the C terminus of PEN-2 are critical for intermolecular interactions and function of presenilin complexes. *J. Biol. Chem.* **279,** 46455–46463
45. Dauch, P., Champigny, G., Ricci, J. E., and Checler, F. (1997) Lack of effect of Presenilin 1, βAPP and their Alzheimer's disease-related mutated forms on *Xenopus* oocytes membrane currents. *Neurosci. Lett.* **221,** 85–88
46. Marambaud, P., Alves da Costa, C., Ancolio, K., and Checler, F. (1998) Alzheimer's disease-linked mutation of presenilin 2 (N141I-PS2) drastically lowers APPα secretion: control by the proteasome. *Biochem. Biophys. Res. Commun.* **252,** 134–138
47. Andrau, D., Dumanchin-Njock, C., Ayral, E., Vizzavona, J., Farzan, M., Boisbrun, M., Fulcrand, P., Hernandez, J.-F., Martinez, J., Lefranc-Jullien, S., and Checler, F. (2003) BACE1- and BACE2-expressing human cells: characterization of β-amyloid precursor protein-derived catabolites, design of a novel fluorimetric assay, and identification of new *in vitro* inhibitors. *J. Biol. Chem.* **278,** 25859–25866
48. Flammang, B., Pardossi-Piquard, R., Sevalle, J., Debayle, D., Dabert-Gay, A.-S., Thévenet, A., Lauritzen, I., and Checler, F. (2012) Evidence that the amyloid-β protein precursor intracellular domain, AICD, derives from β-secretase-generated C-terminal fragment. *J. Alzheimers Dis.* **30,** 145–153
49. Sevalle, J., Amoyel, A., Robert, P., Fournié-Zaluski, M.-C., Roques, B., and Checler, F. (2009) Aminopeptidase A contributes to the N-terminal truncation of amyloid β-peptide. *J. Neurochem.* **109,** 248–256
50. Johnson-Wood, K., Lee, M., Motter, R., Hu, K., Gordon, G., Barbour, R., Khan, K., Gordon, M., Tan, H., Games, D., Lieberburg, I., Schenk, D., Seubert, P., and McConlogue, L. (1997) Amyloid precursor protein processing and Aβ42 deposition in a transgenic mouse model of Alzheimer disease. *Proc. Natl. Acad. Sci. U.S.A.* **94,** 1550–1555
51. Gassmann, M., Grenacher, B., Rohde, B., and Vogel, J. (2009) Quantifying Western blots: pitfalls of densitometry. *Electrophoresis* **30,** 1845–1855
52. Thinakaran, G., Regard, J. B., Bouton, C. M., Harris, C. L., Price, D. L., Borchelt, D. R., and Sisodia, S. S. (1998) Stable association of presenilin derivatives and absence of presenilin interactions with APP. *Neurobiol. Dis.* **4,** 438–453
53. Schägger, H., and von Jagow, G. (1991) Blue native electrophoresis for isolation of membrane protein complexes in enzymatically active form. *Anal. Biochem.* **199,** 223–231
54. Cold Spring Harbor Laboratory (2007) Mowiol-DABCO stock solution. *Cold Spring Harb. Protoc.* 10.1101/pdb.rec10913
55. Ryan, M. D., King, A. M., and Thomas, G. P. (1991) Cleavage of foot-and-mouth disease virus polyprotein is mediated by residues located within a 19 amino acid sequence. *J. Gen. Virol.* **72,** 2727–2732
56. Donnelly, M. L., Luke, G., Mehrotra, A., Li, X., Hughes, L. E., Gani, D., and Ryan, M. D. (2001) Analysis of the aphthovirus 2A/2B polyprotein "cleavage" mechanism indicates not a proteolytic reaction, but a novel translational effect: a putative ribosomal "skip". *J. Gen. Virol.* **82,** 1013–1025
57. Morais, V. A., Crystal, A. S., Pijak, D. S., Carlin, D., Costa, J., Lee, V. M.-Y., and Doms, R. W. (2003) The transmembrane domain region of nicastrin mediates direct interactions with APH-1 and the γ-secretase complex. *J. Biol. Chem.* **278,** 43284–43291
58. Capell, A., Kaether, C., Edbauer, D., Shirotani, K., Merkl, S., Steiner, H., and Haass, C. (2003) Nicastrin interacts with γ-secretase complex components via the N-terminal part of its transmembrane domain. *J. Biol. Chem.* **278,** 52519–52523
59. Acx, H., Chávez-Gutiérrez, L., Serneels, L., Lismont, S., Benurwar, M., Elad, N., and De Strooper, B. (2014) Signature amyloid β profiles are produced by different γ-secretase complexes. *J. Biol. Chem.* **289,** 4346–4355
60. Bergman, A., Laudon, H., Winblad, B., Lundkvist, J., and Näslund, J. (2004) The extreme C terminus of presenilin 1 is essential for γ-secretase complex assembly and activity. *J. Biol. Chem.* **279,** 45564–45572
61. Cheng, H., Vetrivel, K. S., Drisdel, R. C., Meckler, X., Gong, P., Leem, J. Y., Li, T., Carter, M., Chen, Y., Nguyen, P., Iwatsubo, T., Tomita, T., Wong, P. C., Green, W. N., Kounnas, M. Z., and Thinakaran, G. (2009) *S*-Palmitoylation of γ-secretase subunits nicastrin and APH-1. *J. Biol. Chem.* **284,** 1373–1384
62. Kim, S.-H., Ikeuchi, T., Yu, C., and Sisodia, S. S. (2003) Regulated hyperaccumulation of presenilin-1 and the "gamma-secretase" complex: evidence for differential intramembranous processing of transmembrane subatrates. *J. Biol. Chem.* **278,** 33992–34002
63. Lai, M.-T., Chen, E., Crouthamel, M.-C., DiMuzio-Mower, J., Xu, M., Huang, Q., Price, E., Register, R. B., Shi, X.-P., Donoviel, D. B., Bernstein, A., Hazuda, D., Gardell, S. J., and Li, Y.-M. (2003) Presenilin-1 and presenilin-2 exhibit distinct yet overlapping γ-secretase activities. *J. Biol. Chem.* **278,** 22475–22481
64. Lee, J., Song, L., Terracina, G., Bara, T., Josien, H., Asberom, T., Sasikumar, T. K., Burnett, D. A., Clader, J., Parker, E. M., and Zhang, L. (2011) Identification of presenilin 1-selective γ-secretase inhibitors with reconstituted γ-secretase complexes. *Biochemistry* **50,** 4973–4980
65. Gu, Y., Sanjo, N., Chen, F., Hasegawa, H., Petit, A., Ruan, X., Li, W., Shier, C., Kawarai, T., Schmitt-Ulms, G., Westaway, D., St George-Hyslop, P., and Fraser, P. E. (2004) The presenilin proteins are components of multiple membrane-bound complexes that have different biological activities. *J. Biol. Chem.* **279,** 31329–31336
66. Petit, A., Bihel, F., Alvès da Costa, C., Pourquié, O., Checler, F., and Kraus, J. L. (2001) New protease inhibitors prevent γ-secretase-mediated production of Aβ40/42 without affecting Notch cleavage. *Nat. Cell Biol.* **3,** 507–511

67. Pols, M. S., and Klumperman, J. (2009) Trafficking and function of the tetraspanin CD63. *Exp. Cell Res.* **315,** 1584–1592
68. Goodger, Z. V., Rajendran, L., Trutzel, A., Kohli, B. M., Nitsch, R. M., and Konietzko, U. (2009) Nuclear signaling by the APP intracellular domain occurs predominantly through the amyloidogenic processing pathway. *J. Cell Sci.* **122,** 3703–3714
69. Pardossi-Piquard, R., and Checler, F. (2012) The physiology of the β-amyloid precursor protein intracellular domain AICD. *J. Neurochem.* **120,** 109–124
70. Zhang, M., Haapasalo, A., Kim, D. Y., Ingano, L. A. M., Pettingell, W. H., and Kovacs, D. M. (2006) Presenilin/γ-secretase activity regulates protein clearance from the endocytic recycling compartment. *FASEB J.* **20,** 1176–1178
71. Schwarzman, A. L., Singh, N., Tsiper, M., Gregori, L., Dranovsky, A., Vitek, M. P., Glabe, C. G., St George-Hyslop, P. H., and Goldgaber, D. (1999) Endogenous presenilin 1 redistributes to the surface of lamellipodia upon adhesion of Jurkat cells to a collagen matrix. *Proc. Natl. Acad. Sci. U.S.A.* **96,** 7932–7937
72. Ray, W. J., Yao, M., Mumm, J., Schroeter, E. H., Saftig, P., Wolfe, M., Selkoe, D. J., Kopan, R., and Goate, A. M. (1999) Cell surface presenilin-1 participates in the γ-secretase-like proteolysis of Notch. *J. Biol. Chem.* **274,** 36801–36807
73. Leem, J. Y., Vijayan, S., Han, P., Cai, D., Machura, M., Lopes, K. O., Veselits, M. L., Xu, H., and Thinakaran, G. (2002) Presenilin 1 is required for maturation and cell surface accumulation of nicastrin. *J. Biol. Chem.* **277,** 19236–19240
74. Chen, F., Tandon, A., Sanjo, N., Gu, Y.-J., Hasegawa, H., Arawaka, S., Lee, F. J. S., Ruan, X., Mastrangelo, P., Erdebil, S., Wang, L., Westaway, D., Mount, H. T. J., Yankner, B., Fraser, P. E., and St George-Hyslop, P. (2003) Presenilin 1 and presenilin 2 have differential effects on the stability and maturation of nicastrin in mammalian brain. *J. Biol. Chem.* **278,** 19974–19979
75. Iwata, H., Tomita, T., Maruyama, K., and Iwatsubo, T. (2001) Subcellular compartment and molecular subdomain of β-amyloid precursor protein relevant to the Aβ42-promoting effects of Alzheimer mutant presenilin 2. *J. Biol. Chem.* **276,** 21678–21685
76. Dumanchin, C., Czech, C., Campion, D., Cuif, M. H., Poyot, T., Martin, C., Charbonnier, F., Goud, B., Pradier, L., and Frebourg, T. (1999) Presenilins interact with Rab11, a small GTPase involved in the regulation of vesicular transport. *Hum. Mol. Genet.* **8,** 1263–1269
77. Wakabayashi, T., Craessaerts, K., Bammens, L., Bentahir, M., Borgions, F., Herdewijn, P., Staes, A., Timmerman, E., Vandekerckhove, J., Rubinstein, E., Boucheix, C., Gevaert, K., and De Strooper, B. (2009) Analysis of the γ-secretase interactome and validation of its association with tetraspanin-enriched microdomains. *Nature Cell Biol.* **11,** 1340–1346
78. Takeda, K., Araki, W., and Tabira, T. (2004) Enhanced generation of intracellular Aβ42 amyloid peptide by mutation of presenilins PS1 and PS2. *Eur. J. Neurosci.* **19,** 258–264
79. Small, S. A., and Gandy, S. (2006) Sorting through the cell biology of Alzheimer's disease: intracellular pathways to pathogenesis. *Neuron* **52,** 15–31
80. Thinakaran, G., and Koo, E. H. (2008) Amyloid precursor protein trafficking, processing, and function. *J. Biol. Chem.* **283,** 29615–29619
81. Chyung, J. H., and Selkoe, D. J. (2003) Inhibition of receptor-mediated endocytosis demonstrates generation of amyloid β-protein at the cell surface. *J. Biol. Chem.* **278,** 51035–51043
82. Ni, Y., Zhao, X., Bao, G., Zou, L., Teng, L., Wang, Z., Song, M., Xiong, J., Bai, Y., and Pei, G. (2006) Activation of β2-adrenergic receptor stimulates γ-secretase activity and accelerates amyloid plaque formation. *Nat. Med.* **12,** 1390–1396
83. Kamenetz, F., Tomita, T., Hsieh, H., Seabrook, G., Borchelt, D., Iwatsubo, T., Sisodia, S., and Malinow, R. (2003) APP processing and synaptic function. *Neuron* **37,** 925–937
84. Cirrito, J. R., Yamada, K. A., Finn, M. B., Sloviter, R. S., Bales, K. R., May, P. C., Schoepp, D. D., Paul, S. M., Mennerick, S., and Holtzman, D. M. (2005) Synaptic activity regulates interstitial fluid amyloid-β levels *in vivo*. *Neuron* **48,** 913–922
85. Marcello, E., Epis, R., and Di Luca, M. (2008) Amyloid flirting with synaptic failure: towards a comprehensive view of Alzheimer's disease pathogenesis. *Eur. J. Pharmacol.* **585,** 109–118